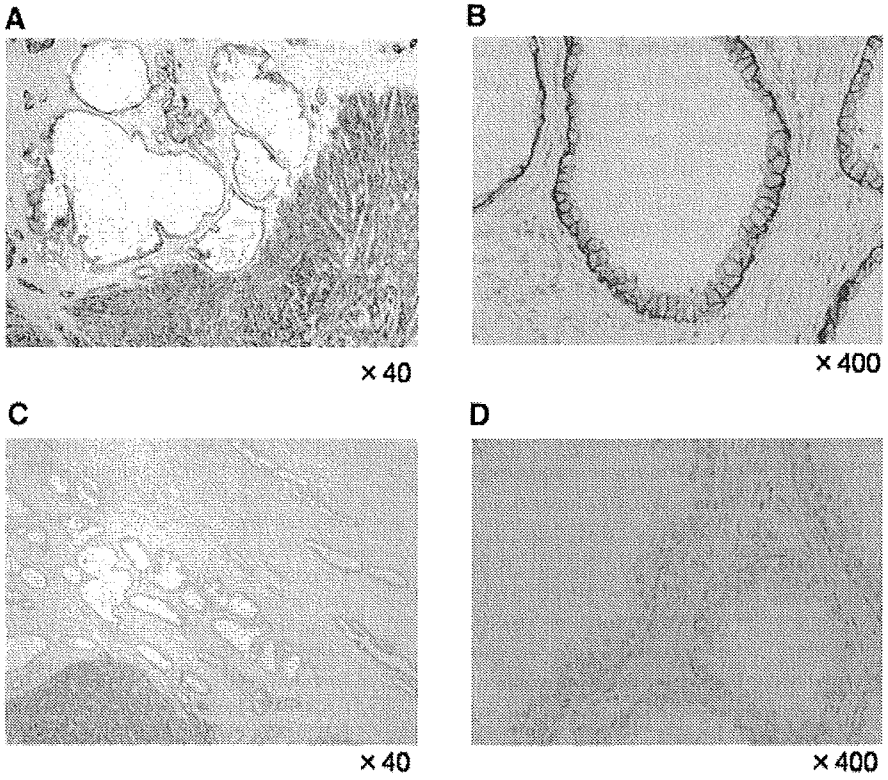

Fig. 8. Immunohistochemical findings for prostate cancer cells and normal epithelial cells of the prostate. **A**: Prostate cancer and normal epithelial cells shows strong immunoreactivity for mAb 1B7. **B**: Basolateral cell surface of normal epithelium shows strong immunoreactivity for mAb 1B7. **C**: Prostate cancer shows strong immunoreactivity for mAb 1B7 but normal epithelial cells do not. **D**: Normal epithelial cells are not stained. Stromal cells are not stained in each sample.

not express PSMA. The first aim of this study is to target adenovirus to resistant cell line PC-3.

We purified four different mAbs and confirmed high transduction efficiency by flow cytometry and chemiluminescent β-Gal reporter gene assay. The target molecules of mAbs 1B7, 2H7, 6F8, and 9B10 were Ep-CAM, CD155, Na,K-ATPase β1, and HAI-1, respectively. CD155 and Na,K-ATPase β1 found to be widely expressed by flow cytometric analysis are inappropriate molecules for tumor targeting. The anti-Ep-CAM antibody mAb 1B7 and anti-HAI-1 antibody mAb 2H7 showed reactivity with cancer cell lines other than fibroblast cell lines. We could not find reactivity with prostate cancer samples for mAb 2H7, 6F8, or 9B10. These mAbs may be unsuitable for staining of samples fixed in formalin. In mAb 1B7, we found that Ep-CAM expression on prostate cancer cells was stronger than on normal epithelial cells, but not significantly. In 1979, Ep-CAM was discovered in a search for novel cell surface antigens expressed on neoplastic tissue [18]. Ep-CAM is known to be expressed on the basolateral cell surfaces of selected normal epithelia and many carcinomas [19–22]. Of particular interest, overexpression of Ep-CAM has been reported in prostate cancer [21,23]. Clinical trials of mAbs directed against Ep-CAM for immunologic therapy have been conducted in patients with colon cancer [24]. Recently, clinical phase I study with anti-Ep-CAM humanized IgG1 have been performed in patients with hormone refractory prostate cancer by Oberneder et al. [25]. Heideman et al. [26] showed that Ep-CAM targeted vectors using bispecific antibodies against the adenovirus fiber-knob protein, and Ep-CAM may be useful for gastric and esophageal cancer-specific gene therapy. HAI-1 is a novel Kunitz-type serine protease inhibitor first reported in 1997 [27]. Although, HAI-1 is broadly expressed in epithelial cells of most human tissues [28,29], Knudsen et al. [30] reported that its expression was significantly increased in localized prostate cancer and was present in most prostate cancer metastases compared to normal prostate glands. Furthermore, HAI-1 overexpression in prostate cancer was predictive of prostate-specific antigen recurrence. Nagakawa et al. [31] demonstrated that significantly increased serum levels of HAI-1 were detected in patients with prostate cancer, indicating that HAI-1

would be a potential tumor marker for prostate cancer. Ep-CAM and HAI-1 overexpressed in prostate cancer may be potential targets for prostate cancer gene therapy with Adv-FZ33, although therapeutic effectiveness must be evaluated as well. In future clinical application, we would like to use Adv-FZ33 premixed with prostate cancer targeting mAb prior to injection. This method seems to be more practical for administration systemically.

In addition to mAb 1B7 and 9B10, we may be able to establish new prostate cancer-specific mAbs through the hybridoma screening system that was designed in this study. Previously, Lampe et al. [32] performed fusions 25 times and developed three mAb directed against prostate associated antigens that might identify potential new therapeutic targets through screening of circa 25,000–50,000 hybridomas. We evaluated only 2,500 wells through three fusions and identified potential four target molecules. Overall, this approach of inductive method using FZ33 fiber-modified adenovirus is reliable strategy for screening useful mAbs that recognize target molecules in prostate cancer gene therapy as well as antibody therapy and diagnosis.

CONCLUSIONS

We established hybridoma from mice immunized with prostate cancer cell lines and selected anti-Ep-CAM mAb and anti-HAI-1 mAbs. Using Adv-FZ33, these mAbs increased transduction efficiency to prostate cancer cells. Gene transduction via Ep-CAM and HAI-1 may be a novel strategy for treatment of prostate cancer.

ACKNOWLEDGMENTS

The authors thank Ms. Toshie Kurohata for her technical assistance. This study was partly supported by the Stiftelsen Japanese-Swedish Cooperative Foundation (T. Tsukamoto), by Grant-in-Aid for Cancer Research from the Ministry of Health and Welfare of Japan (K. Kato and H. Hamada) and by Grant-in-Aid for Scientific Research on Priority Areas "Cancer" from the Ministry of Education, Culture, Sports, Science and Technology (K. Kato, K. Nakamura, and H. Hamada).

REFERENCES

1. Jemal A, Thomas A, Murray T, Thun M. Cancer statistics. CA Cancer J Clin 2002;52:23–47.
2. Kasper S, Cookson MS. Mechanism leading to the development of hormone-resistant prostate cancer. Urol Clin N Am 2006;33: 201–210.
3. Macrae EJ, Giannoudis A, Ryan R, Brown NJ, Hamdy FC, Maitland N, Lewis CE. Gene therapy for prostate cancer: Current strategies and new cell-based approaches. Prostate 2006;66:470–494.
4. Brody SL, Crystal RG. Adenovirus-mediated in vivo gene transfer. Ann N Y Acad Sci 1994;716:90–101; (discussion 101–103).
5. Bergelson JM, Cunningham JA, Droguett G, Kurt-Jones EA, Krithivas A, Hong JS, Horwitz MS, Crowell RL, Finberg RW. Isolation of a common receptor for Coxsackie B viruses and adenoviruses 2 and 5. Science 1997;275:1320–1323.
6. Volpers C, Thirion C, Biermann V, Hussmann S, Kewes H, Dunant P, von der Mark H, Herrmann A, Kochanek S, Lochmuller H. Antibody-mediated targeting of an adenovirus vector modified to contain a synthetic immunoglobulin g-binding domain in the capsid. J Virol 2003;77:2093–2104.
7. Hisataki T, Itoh N, Suzuki K, Takahashi A, Masumori N, Tohse N, Ohmori Y, Yamada S, Tsukamoto T. Modulation of phenotype of human prostatic stromal cells by transforming growth factor-betas. Prostate 2004;58:174–182.
8. Tanaka T, Huang J, Hirai S, Kuroki M, Kuroki M, Watanabe N, Tomihara K, Kato K, Hamada H. Carcinoembryonic antigen-targeted selective gene therapy for gastric cancer through FZ33 fiber-modified adenovirus vectors. Clin Cancer Res 2006;12: 3803–3813.
9. Kitamura H, Torigoe T, Asanuma H, Hisasue SI, Suzuki K, Tsukamoto T, Satoh M, Sato N. Cytosolic overexpression of p62 sequestosome 1 in neoplastic prostate tissue. Histopathology 2006;48:157–161.
10. Getzenberg RH, Abrahamsson PA, Canto EI, Chinnaiyan AM, Djavan B, Laxman B, Ogawa O, Slawin K, Tomlins SA, Yu J. Advances in biomarkers for prostatic disease. In: McConnell J, Denis L, Akaza H, Khoury S, Schalken J, editors. Prostate Cancer. Paris: Health Publications; 2006. pp 85–148.
11. Lieberman R. Evidence-based medical perspectives: The evolving role of PSA for early detection, monitoring of treatment response, and as a surrogate end point of efficacy for interventions in men with different clinical risk states for the prevention and progression of prostate cancer. Am J Ther 2004;11:501–506.
12. Migita T, Oda Y, Naito S, Morikawa W, Kuwano M, Tsuneyoshi M. The accumulation of angiostatin-like fragments in human prostate carcinoma. Clin Cancer Res 2001;7:2750–2756.
13. Horoszewicz JS, Kawinski E, Murphy GP. Monoclonal antibodies to a new antigenic marker in epithelial prostatic cells and serum of prostatic cancer patients. Anticancer Res 1987;7:927–935.
14. Israeli RS, Powell CT, Corr JG, Fair WR, Heston WD. Expression of the prostate-specific membrane antigen. Cancer Res 1994;54: 1807–1811.
15. Sokoloff RL, Norton KC, Gasior CL, Marker KM, Grauer LS. A dual-monoclonal sandwich assay for prostate-specific membrane antigen: Levels in tissues, seminal fluid and urine. Prostate 2000;43:150–157.
16. Janssen T, Darro F, Petein M, Raviv G, Pasteels JL, Kiss R, Schulman CC. In vitro characterization of prolactin-induced effects on proliferation in the neoplastic LNCaP, DU145, and PC-3 models of the human prostate. Cancer 1996;77:144–149.
17. Okegawa T, Li Y, Pong RC, Bergelson JM, Zhou J, Hsieh JT. The dual impact of coxsackie and adenovirus receptor expression on human prostate cancer gene therapy. Cancer Res 2000;60:5031–5036.
18. Herlyn M, Steplewski Z, Herlyn D, Koprowski H. Colorectal carcinoma-specific antigen: Detection by means of monoclonal antibodies. Proc Natl Acad Sci USA 1979;76:1438–1442.
19. Momburg F, Moldenhauer G, Hammerling GJ, Moller P. Immunohistochemical study of the expression of a Mr 34,000

human epithelium-specific surface glycoprotein in normal and malignant tissues. Cancer Res 1987;47:2883–2891.

20. Xie X, Wang CY, Cao YX, Wang W, Zhuang R, Chen LH, Dang NN, Fang L, Jin BQ. Expression pattern of epithelial cell adhesion molecule on normal and malignant colon tissues. World J Gastroenterol 2005;11:344–347.
21. Went P, Vasei M, Bubendorf L, Terracciano L, Tornillo L, Riede U, Kononen J, Simon R, Sauter G, Baeuerle PA. Frequent high-level expression of the immunotherapeutic target Ep-CAM in colon, stomach, prostate and lung cancers. Br J Cancer 2006;94: 128–135.
22. Heinzelmann-Schwarz VA, Gardiner-Garden M, Henshall SM, Scurry J, Scolyer RA, Davies MJ, Heinzelmann M, Kalish LH, Bali A, Kench JG, Edwards LS, Vanden Bergh PM, Hacker NF, Sutherland RL, O'Brien PM. Overexpression of the cell adhesion molecules DDR1, claudin 3, and Ep-CAM in metaplastic ovarian epithelium and ovarian cancer. Clin Cancer Res 2004;10:4427–4436.
23. Poczatek RB, Myers RB, Manne U, Oelschlager DK, Weiss HL, Bostwick DG, Grizzle WE. Ep-Cam levels in prostatic adenocarcinoma and prostatic intraepithelial neoplasia. J Urol 1999; 162:1462–1466.
24. Mosolits S, Nilsson B, Mellstedt H. Towards therapeutic vaccines for colorectal carcinoma: A review of clinical trials. Expert Rev Vaccines 2005;4:329–350.
25. Oberneder R, Weckermann D, Ebner B, Quadt C, Kirchinger P, Raum T, Locher M, Prang N, Baeuerle PA, Leo E. A phase I study with adecatumumab, a human antibody directed against epithelial cell adhesion molecule, in hormone refractory prostate cancer patients. Eur J Cancer 2006;42:2530–2538.
26. Heideman DA, Snijders PJ, Craanen ME, Bloemena E, Meijer CJ, Meuwissen SG, van Beusechem VW, Pinedo HM, Curiel DT, Haisma HJ, Gerritsen WR. Selective gene delivery toward gastric and esophageal adenocarcinoma cells via EpCAM-targeted adenoviral vectors. Cancer Gene Ther 2001;8:342–351.
27. Shimomura T, Denda K, Kitamura A, Kawaguchi T, Kito M, Kondo J, Kagaya S, Qin L, Takata H, Miyazawa K, Kitamura N. Hepatocyte growth factor activator inhibitor, a novel Kunitz-type serine protease inhibitor. J Biol Chem 1997;272:6370–6376.
28. Kataoka H, Suganuma T, Shimomura T, Itoh H, Kitamura N, Nabeshima K, Koono M. Distribution of hepatocyte growth factor activator inhibitor type 1 (HAI-1) in human tissues. Cellular surface localization of HAI-1 in simple columnar epithelium and its modulated expression in injured and regenerative tissues. J Histochem Cytochem 1999;47:673–682.
29. Oberst M, Anders J, Xie B, Singh B, Ossandon M, Johnson M, Dickson RB, Lin CY. Matriptase and HAI-1 are expressed by normal and malignant epithelial cells in vitro and in vivo. Am J Pathol 2001;158:1301–1311.
30. Knudsen BS, Lucas JM, Fazli L, Hawley S, Falcon S, Coleman IM, Martin DB, Xu C, True LD, Gleave ME, Nelson PS, Ayala GE. Regulation of hepatocyte activator inhibitor-1 expression by androgen and oncogenic transformation in the prostate. Am J Pathol 2005;167:255–266.
31. Nagakawa O, Yamagishi T, Akashi T, Nagaike K, Fuse H. Serum hepatocyte growth factor activator inhibitor type I (HAI-I) and type 2 (HAI-2) in prostate cancer. Prostate 2006;66:447–452.
32. Lampe MI, Molkenboer-Kuenen JD, Oosterwijk E. Development of new prostate specific monoclonal antibodies. Prostate 2004; 58:225–231.

THE JOURNAL OF BIOLOGICAL CHEMISTRY VOL. 284, NO. 38, pp. 25585–25592, September 18, 2009

Translesional DNA Synthesis through a C8-Guanyl Adduct of 2-Amino-1-methyl-6-phenylimidazo[4,5-*b*]pyridine (PhIP) *in Vitro*

REV1 INSERTS dC OPPOSITE THE LESION, AND DNA POLYMERASE κ POTENTIALLY CATALYZES EXTENSION REACTION FROM THE 3′-dC TERMINUS[*][S]

Received for publication, June 25, 2009, and in revised form, July 16, 2009 Published, JBC Papers in Press, July 23, 2009, DOI 10.1074/jbc.M109.037259

Hirokazu Fukuda[‡], Takeji Takamura-Enya[§], Yuji Masuda[¶], Takehiko Nohmi[‖], Chiho Seki[‡], Kenji Kamiya[¶], Takashi Sugimura[‡], Chikahide Masutani[**], Fumio Hanaoka[1], and Hitoshi Nakagama[‡2]**

From the [‡]Biochemistry Division, National Cancer Center Research Institute, 1-1, Tsukiji 5, Chuo-ku, Tokyo 104-0045, the [§]Department of Applied Chemistry, Faculty of Engineering, Kanagawa Institute of Technology, Ogino 1030, Atsugi, Kanagawa 243-0292, the [¶]Department of Experimental Oncology, Research Institute for Radiation Biology and Medicine, Hiroshima University, Kasumi 1-2-3, Minami-ku, Hiroshima, Hiroshima 734-8553, the [‖]Division of Genetics and Mutagenesis, National Institute of Health Sciences, Kamiyoga 1-18-1, Setagaya-ku, Tokyo 158-8501, and the [**]Cellular Biology Laboratory, Graduate School of Frontier Biosciences, Osaka University, Yamada-oka 1-3, Suita, Osaka 565-0871, Japan

2-Amino-1-methyl-6-phenylimidazo[4,5-*b*]pyridine (PhIP) is the most abundant heterocyclic amine in cooked foods, and is both mutagenic and carcinogenic. It has been suspected that the carcinogenicity of PhIP is derived from its ability to form DNA adducts, principally dG-C8-PhIP. To shed further light on the molecular mechanisms underlying the induction of mutations by PhIP, *in vitro* DNA synthesis analyses were carried out using a dG-C8-PhIP-modified oligonucleotide template. In this template, the dG-C8-PhIP adduct was introduced into the second G of the TCC GGG AAC sequence located in the 5′ region. This represents one of the mutation hot spots in the rat *Apc* gene that is targeted by PhIP. Guanine deletions at this site in the *Apc* gene have been found to be preferentially induced by PhIP in rat colon tumors. DNA synthesis with A- or B-family DNA polymerases, such as *Escherichia coli* polymerase (pol) I and human pol δ, was completely blocked at the adducted guanine base. Translesional synthesis polymerases of the Y-family, pol η, pol ι, pol κ, and REV1, were also used for *in vitro* DNA synthesis analyses with the same templates. REV1, pol η, and pol κ were able to insert dCTP opposite dG-C8-PhIP, although the efficiencies for pol η and pol κ were low. pol κ was also able to catalyze the extension reaction from the dC opposite dG-C8-PhIP, during which it often skipped over one dG of the triple dG sequence on the template. This slippage probably leads to the single dG base deletion in colon tumors.

Heterocyclic amines (HCAs)[3] are naturally occurring genotoxic carcinogens produced from cooking meat (1). The initial carcinogenic event induced by HCAs is metabolic activation and subsequent covalent bond formation with DNA (1, 2). 2-Amino-1-methyl-6-phenylimidazo[4,5-*b*]pyridine (PhIP) is the most abundant heterocyclic amine in cooked foods, and was isolated from fried ground beef (3, 4). PhIP possesses both mutagenic and carcinogenic properties (5–8). Epidemiological studies have revealed that a positive correlation exists between PhIP exposure and mammary cancer incidence (9). PhIP induces colon and prostate cancers in male rats and breast cancer in female rats (8, 10).

The incidences of colon, prostate, and breast cancers are steadily increasing in Japan and other countries and this has been found to correlate with a more Westernized lifestyle. Elucidating the molecular mechanisms underlying PhIP-induced mutations is therefore of considerable interest. It is suspected that the carcinogenicity of PhIP is derived from the formation of DNA adducts, principally dG-C8-PhIP (11–14) (see Fig. 1). Studies of the mutation spectrum of PhIP in mammalian cultured cells and transgenic animals have revealed that G to T transversions are predominant and that guanine deletions from G stretches, especially from the 5′-GGGA-3′ sequence, are significant (15–20). Five mutations in the *Apc* gene were detected in four of eight PhIP-induced rat colon tumors, and all of these mutations involved a single base deletion of guanine from 5′-GGGA-3′ (21). These mutation spectra are thought to be influenced by various factors, including the primary structure of the target gene itself, the capacity of translesional DNA polymerases, and the activity level of repair enzymes (1). However, the molecular mechanisms underlying the formation of PhIP-induced mutations are largely unknown.

To shed further light on the molecular processes that underpin the mutations induced by PhIP, we performed *in vitro* DNA synthesis analyses using a dG-C8-PhIP-modified oligonucleotide template. We have recently reported the successful synthesis of oligonucleotides harboring a site-specific PhIP adduct

* This work was supported by Kakenhi Grant 19570144.
[S] The on-line version of this article (available at http://www.jbc.org) contains supplemental Table S1 and Figs. S1–S6.
[1] Present address: Dept. of Life Science, Faculty of Science, Gakushuin University, Mejiro 1-5-1, Toshima-ku, Tokyo 171-8588, Japan.
[2] To whom correspondence should be addressed. Tel.: 81-3-3542-2511; Fax: 81-33542-2530; E-mail: hnakagam@ncc.go.jp.
[3] The abbreviations used are: HCA, heterocyclic amines; PhIP, 2-amino-1-methyl-6-phenylimidazo[4,5-*b*]pyridine; TLS, translesional DNA synthesis; IQ, 2-amino-3-methylimidazo[4,5-*f*]quinoline; pol, DNA polymerase; DTT, dithiothreitol; PCNA, proliferating cell nuclear antigen; PIPES, 1,4-piperazinediethanesulfonic acid.

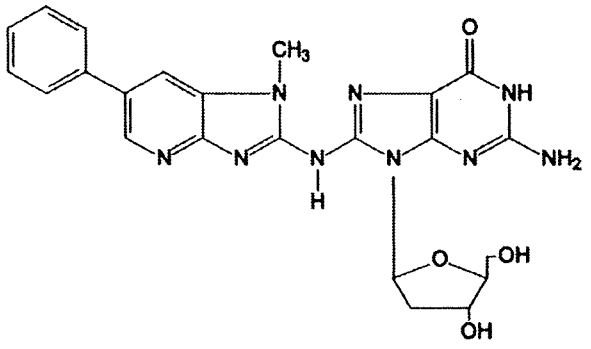

dG-C8-PhIP

FIGURE 1. **Structure of the dG-C8-PhIP adduct.**

(22). In our current study, we used this synthesis method to construct a 32-mer oligonucleotide template containing a 5′-TTCGGGAAC-3′ sequence with different site-specific PhIP adducts. We then utilized the resulting constructs in DNA synthesis analyses to reconstitute the PhIP-induced mutagenesis of the rat *APC* gene. DNA synthesis reactions with A- or B-family DNA polymerases, such as *Escherichia coli* pol I and human pol δ, or translesional synthesis (TLS) polymerases of the Y-family, pol η, pol ι, pol κ, and REV1, were carried out. Kinetic analyses of pol κ and REV1, for which TLS activities at the PhIP adduct were detected, were also performed.

EXPERIMENTAL PROCEDURES

Enzymes and Materials—T4 polynucleotide kinase and T4 DNA ligase were purchased from Toyobo Biochem (Osaka, Japan) and Takara Biotech (Tokyo Japan), respectively. Other materials were obtained from Sigma or Wako (Osaka, Japan).

DNA Polymerases and PCNA—Human recombinant DNA polymerases, pol δ, pol η, pol κ, and REV1, and PCNA were expressed and purified as described previously (23–27). Human DNA polymerase α and DNA polymerase ι were purchased from Chimerx. *E. coli* DNA polymerases I (Takara Biotech) and Klenow Fragment (Takara Biotech), and thermophilic bacterial DNA polymerases, r*Taq* (Toyobo Biochem) and *Tth* (Toyobo Biochem) were used.

Oligonucleotides—The method used to chemically synthesize three 9-mer oligonucleotides, 5′-TCCGGGAAC-3′, containing a PhIP adduct on either the first, second, or third G (p9B, p9C, and p9D, respectively) has been described previously (22). All other synthetic oligonucleotides were synthesized and purified using a reverse-phase cartridge (Operon Biotech Japan (Tokyo, Japan). The 23-mer oligonucleotides: p23a, 5′-TGACTCGTCGTGACTGGGAAAAC-3′, and p23b, 5′-GTCACGACGAGTCAGTTCCCGGA-3′, were used for constructing the template oligonucleotides as described below. A 32-mer oligonucleotide without the PhIP adduct, p32A, was used as a control template (see Table 1). Its 3′ complementary 29-, 28-, 27-, 26-, 22-, and 17-mer sequences (p29, p28, p27, p26, p22, and p17) were used as extension primers (see Table 1).

Construction of Template-Primer Complexes Containing the PhIP Adduct—A 32-mer template oligonucleotide p32C (see Table 1) was constructed by ligation of p9C with p23a as follows. The 5′-end of p23a was phosphorylated by T4 polynucleotide kinase and ATP. A mixture of p9C, p23a, and p23b (3 nmol each) in 250 μl of a buffer containing 5 mM Tris-HCl, 0.5 mM EDTA, 50 mM NaCl, pH 8.0, was denatured for 5 min at 95 °C, incubated for 10 min at 60 °C, and then cooled slowly to form the partial duplex structure of these three oligonucleotides (supplemental Fig. S1). The sample of the duplex oligonucleotide was mixed with 190 μl of Milli-Q water and 50 μl of ×10 ligation buffer (500 mM Tris-HCl (pH 7.5), 100 mM $MgCl_2$, 100 mM DTT, 10 mM ATP). Ligation was initiated by adding 10 μl of T4 DNA ligase (4,000 units), and the mixture was then incubated for 20 h at 16 °C. An additional incubation at 37 °C for 60 min was carried out after the addition of 1 μl of T4 DNA ligase, and the reaction was stopped by further incubation at 68 °C for 10 min. The p32C was separated by 18% PAGE containing 8 M urea, and excised and eluted as described previously (28). p32B and p32D were constructed using a similar method as for p9B and p9D, respectively (see Table 1). The purities of these oligonucleotides, p32B, p32C, and p32D, were determined by denatured PAGE after 5′-end labeling and UV absorbance at 260 and 370 nm.

Primer oligonucleotides were labeled with ^{32}P at the 5′-end as described previously (29), and then purified by MicroSpin™ G-25 or G-50 columns (GE Healthcare) as recommended by the supplier. The mixture of template and labeled primer (50 pmol each) in 400 μl of a buffer containing 8 mM Tris-HCl, 0.8 mM EDTA, 150 mM KCl (pH 8.0) was heated at 70 °C for 7 min, and then cooled slowly to room temperature. In the case of the substrates for TLS polymerases, pol η, pol ι, pol κ, and REV1, the final concentrations of template-primer and the constituents of the annealing buffers were changed to 500 nM and 10 mM Tris-HCl, 1 mM EDTA, and 50 mM NaCl (pH 8.0), respectively.

In Vitro DNA Synthesis Assay—A primer extension reaction was performed as described previously (30) with some modifications. Briefly, an aliquot of 0.75 μl of this primer-annealed template (final concentration, 12.5 nM) was mixed with 0.75 μl of ×10 Klenow buffer (100 mM Tris-HCl (pH 7.5), 70 mM $MgCl_2$, 1 mM DTT), 0.5 μl of 500 mM KCl, 0.5 μl of dNTP mixture (50 μM each), and 4.5 μl of Milli-Q water. After addition of 0.5 μl of Klenow fragment, the mixture was incubated at 37 °C for 10 min. The reaction was terminated by adding 1.5 μl of stop solution (160 mM EDTA, 0.7% SDS, 6 mg/ml proteinase K), and the samples were incubated at 37 °C for 30 min. Subsequently, 5.5 μl of the gel loading solution (30 mM EDTA, 0.05% bromophenol blue, 0.05% xylene cyanol, 97% formamide) was added to the samples. For pol δ, a ×10 reaction buffer containing 200 mM PIPES (pH 6.8), 20 mM $MgCl_2$, 10 mM 2-mercaptethanol, 200 μg/ml bovine serum albumin, and 50% glycerol was used instead of the buffer described above, and the reaction was carried out at 37 °C for 10 min. For other DNA polymerases, pol α, pol I, r*Taq*, and *Tth*, the constituent of each ×10 reaction buffer was altered as recommended by the suppliers.

The reaction using pol κ was performed as described above with some modifications. Briefly, an aliquot of 0.5 μl of this primer-annealed template (final 50 nM) was mixed with 0.5 μl of 10 × TLS buffer (250 mM Tris-HCl (pH 7.0), 50 mM $MgCl_2$, 50 mM DTT, 1 mg/ml bovine serum albumin), 0.5 μl of dNTP solution, and 3.0 μl of Milli-Q water. After addition of 0.5 μl of pol κ, the mixture was incubated at 30 °C for 20 min. The reac-

tion was terminated by adding 8.8 μl of the gel loading solution and a further incubation at 95 °C for 3 min. The reaction of REV1 was performed in the same manner as the reaction of pol κ with the exception that the standard reaction time was 5 min. For pol η, a ×10 reaction buffer containing 400 mM Tris-HCl (pH 8.0), 10 mM $MgCl_2$, 100 mM DTT, 1 mg/ml bovine serum albumin, and 450 mM KCl was used instead of the ×10 TLS buffer. The ^{32}P-labeled fragments were denatured and electrophoresed in a 9.5% polyacrylamide gel containing 8 M urea. The radioactivity of the fragments was determined using a Bio-Imaging Analyzer (BAS2500, Fuji Photo Film, Kanagawa, Japan). Kinetic parameters were determined by steady-state gel kinetic assays under similar conditions as described above. The incubation time for pol κ was changed to 10 min. K_m and k_{cat} were evaluated from the plot of the initial velocity *versus* the dCTP or dGTP concentration using a hyperbolic curve-fitting program in SigmaPlot 11 (Systat Software, Inc.). Data from two or three independent experiments were plotted together.

RESULTS

Construction of Template Oligonucleotides Containing a PhIP Adduct—We designed oligonucleotides containing a dG-C8-PhIP adduct at specific sites for use as templates in *in vitro* DNA synthesis analyses. For this purpose, we selected the 5′-TCCGGGAAC-3′ sequence as: 1) it corresponds to codon 868 – 870 of the rat *Apc* gene, one of three mutation hot spots (a single base deletion of G) in PhIP-induced colon tumors (21), and could thus be used as a model template that would reconstitute mutations of this gene; 2) two other mutation hot spots in the rat *Apc* gene and many mutated sites induced by PhIP in cultured cells and animal models contain 5′-GGGA-3′ as a core sequence (17–20). We thus speculated that the 5′-TCCGGGAAC-3′ sequence could be used as a model sequence for these GGGA to GGA mutations to some extent; and 3) some mutagenic compounds forming dG adducts, including PhIP, are expected to react preferentially with the 5′-G of a GG dinucleotide site when compared with a single G residue (31). We thus selected a sequence containing GGG as a template for our initial analysis.

We have recently synthesized three 9-mer oligonucleotides separately harboring a PhIP adduct on each G within the sequence 5′-TCC GGG AAC-3′ (22). Three 32-mer template oligonucleotides, p32B, p32C, and p32D, were constructed in our present study by ligation of these 9-mer oligonucleotides containing the dG-PhIP adduct with a 23-mer oligonucleotide, p23a, (Table 1 and supplemental Fig. S1). The purities of these oligonucleotides were tested after resolution by electrophoresis. In our present study, we principally describe the results of our *in vitro* DNA synthesis analysis using p32C as the template to avoid complexity.

In Vitro DNA Synthesis by A- and B-family DNA Polymerase—Many of the chemical compounds that can form DNA adducts *in vivo* and that show mutagenicity have been reported to impede the progress of DNA synthesis to different extents. The molecular size of PhIP is greater than most other mutagenic chemicals that form adducts. Hence, dG-PhIP was expected to block DNA synthesis to a considerable extent. To examine the effects of the dG-C8-PhIP adduct upon DNA synthesis, primer

TABLE 1
Oligonucleotide templates and primers

Oligonucleotide	Sequence[a]
p32A	5′-TCC GGG AAC TGACTCGTC GTGACTGGG AAAAC-3′
p32B	5′-TCC **G**GG AAC TGACTCGTC GTGACTGGG AAAAC-3′
p32C	5′-TCC G**G**G AAC TGACTCGTC GTGACTGGG AAAAC-3′
p32D	5′-TCC GG**G** AAC TGACTCGTC GTGACTGGG AAAAC-3′
p29	5′-GTT TTC CCA GTCACGACG AGTCAGTTC CC-3′
p28	5′-GTT TTC CCA GTCACGACG AGTCAGTTC C-3′
p27	5′-GTT TTC CCA GTCACGACG AGTCAGTTC-3′
p26	5′-GTT TTC CCA GTCACGACG AGTCAGTT-3′
p22	5′-GTT TTC CCA GTCACGACG AGTC-3′
p17	5′-GTT TTC CCA GTCACGAC-3′

[a] The bold G indicates the site of the PhIP-C8-dG adduct. Underlined sequences correspond to codon 868 – 870 at nucleotides 2602–2610 of the rat APC gene.

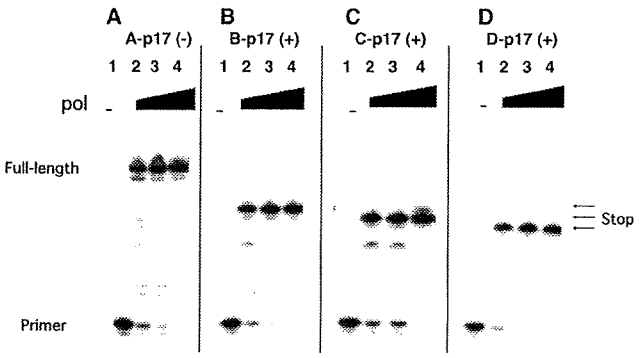

FIGURE 2. ***In vitro* DNA synthesis using Klenow fragment.** Gel electrophoresis indicating the primer extensions obtained using the 32-mer oligonucleotide templates, p32A (*A*), p32B (*B*), p32C (*C*), and p32D (*D*), which have no PhIP adduct, and a PhIP adduct on the first, second, and third G within the triple G sequence, respectively. The 3′ complementary 17-mer sequence, p17, was used as the extension primer. The final concentration of each template-primer complex was 12.5 nM. Concentrations of Klenow fragment were 0 (*lane 1*), 7.8 (*lane 2*), 23 (*lane 3*), and 78 units/ml (*lane 4*).

extension experiments using p32B, p32C, and p32D as templates were carried out (see Table 1). The length of each produced fragment was precisely determined using ladders of oligonucleotide fragments as markers (data not shown). The Klenow fragment of *E. coli* DNA polymerase I, a member of the A-family DNA polymerases, was first used in this analysis. The production of a 28-, 27-, and 26-mer from these primer extension reactions using B-p17, C-p17, and D-p17, respectively, using a template-primer complex, and lack of longer fragments indicated that the Klenow fragment stalled just before the dG-C8-PhIP adduct (Fig. 2). On the other hand, control experiments using p32A without the adduct as a template produced a 32-mer fragment (Fig. 2*A*). Similar results were obtained with *E. coli* DNA polymerase I (exo$^+$) and B-family DNA polymerases, such as the thermophilic bacterial DNA polymerases, r*Taq* and *Tth*, and human DNA polymerase α (data not shown) (supplemental Fig. S2), suggesting that stalling at the dG-C8-PhIP adduct occurs for all replicative DNA polymerases. Stalling of r*Taq* and *Tth* at the PhIP adduct was observed at 65 °C, as well as at 37 °C, indicating that this is the result of a physical hindrance of the adduct itself and not from secondary DNA structures. Moreover, there was no difference found between the stalling of *E. coli* DNA polymerase I (exo$^+$) and that of the Klenow fragment (exo$^-$). This indicates that the physical blocking of DNA polymerases at the dG-C8-PhIP adduct does not depend upon their proofreading function.

Finally, DNA synthesis analyses with human DNA polymerase δ (pol δ), a member of the B-family DNA polymerases and a truly replicative polymerase, were carried out. In the case of using p32C and p17 (C-p17) as a template-primer complex, the production of 27-mer fragments indicated the stalling of pol δ just before the PhIP adduct (Fig. 3, *lane 11*). From a control reaction using A-p17, a template-primer complex without the PhIP adduct, a full-length product of 32-mer was generated (Fig. 3, *lane 8*). In addition to these major products, minor products extended one nucleotide further (28- and 33-mer) and ladders of bands indicating degradation of primer (<17-mer) were observed (Fig. 3), corresponding with previous results reporting terminal dA transferase and exonuclease activities of pol δ (32). PCNA, an accessory protein acting as a sliding clamp for pol δ, was previously reported to promote DNA synthesis by pol δ past several template lesions, including abasic sites, 8-oxo-dG, and aminofluorene-dG (32). In the case of dG-C8-PhIP, however, PCNA was unable to promote the bypass synthesis of pol δ beyond the lesion (Fig. 3, *lane 12*). Extension reaction from the longer 22-mer primer, p22, also paused completely just before the PhIP adduct in the presence or absence of PCNA (Fig. 3, *lanes 5* and *6*). These results strongly suggest that the dG-C8-PhIP adduct on genome DNA in the living cells induces the complete block of replication forks including pol δ, PCNA, and pol α.

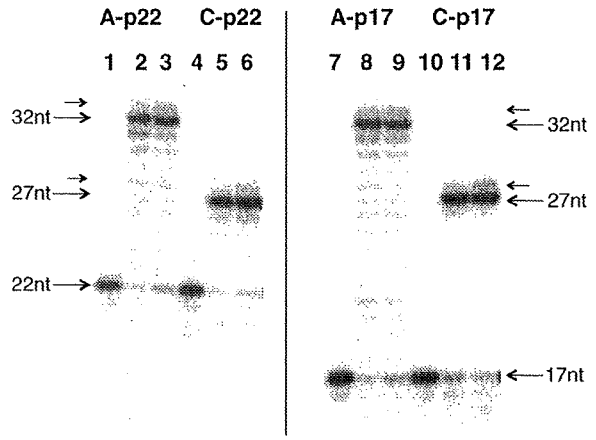

FIGURE 3. ***In vitro* DNA synthesis using pol δ in the presence or absence of PCNA.** Gel electrophoresis indicating the primer extensions obtained using the 32-mer oligonucleotide templates, p32A (*A*), and p32C (*C*), which have no PhIP adduct, and a PhIP adduct on the second G within the triple G sequence, respectively. The 3′ complementary 22- and 17-mer sequences, p22 and p17, were used as the extension primer. The final concentration of each template-primer complex was 12.5 nM. Concentrations of pol δ were 0 (*lanes 1, 4, 7,* and *10*) and 16 nM (*lanes 2, 3, 5, 6, 8, 9, 11,* and *12*). Concentrations of PCNA as a trimer were 0 (*lanes 1, 2, 4, 5, 7, 8, 10,* and *11*) and 20 nM (*lanes 3, 6, 9,* and *12*). *Large arrows* indicate the positions of primers (17- or 22-mer), full-length products (32-mer), and the products pausing just before the PhIP adduct (27-mer). *Small arrows* indicate the minor products that incorporated an additional 1 nucleotide (*nt*) to a full-length product or the pausing product.

Translesional DNA Synthesis by Y-family DNA Polymerases—Translesional DNA synthesis at the dG-C8-PhIP adduct by the Y-family DNA polymerases, pol η, pol κ, pol ι, and REV1 was next examined. Two substrates, C-p27 and C-p28, and their counterparts without a PhIP adduct, A-p27 and A-p28, were used in these experiments (Fig. 4). Substrate C-p27 was prepared by annealing the p32C template (see Table 1) to its 3′-complimentary 27-mer sequence, p27, and was used to identify the nucleotides that are inserted opposite the dG-C8-PhIP adduct (Fig. 4). Similarly, substrate C-p28 was used to analyze the extension reaction from the 3′-end of the dC bases opposite the dG-C8-PhIP adduct (Fig. 4). We found that recombinant human DNA polymerase η (pol η) could insert a dC opposite the dG-C8-PhIP adduct, although at low efficiency compared with control experiments without the PhIP adduct (Fig. 5, *A* and *B*). Extension reactions catalyzed by pol η from the 3′-end of dC opposite the adduct were barely detectable (Fig. 5*D*), although an excessive amount of pol η produced byproducts that incorporated a mismatch nucleotide, dG, dA, or dT (supplemental Fig. S4). In the case of dG, incorporation of one to three dG nucleotides was observed (supplemental Fig. S4). In control experiments without the PhIP adduct, minor products were produced that incorporated mismatch nucleotides, in addition to a major product that incorporated a dC (Fig. 5*C*).

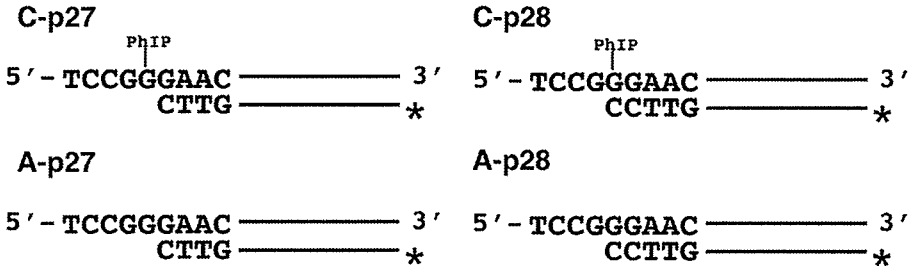

FIGURE 4. **Template-primer complexes.** Substrates C-p27 and C-p28 (series-C) have a PhIP adduct on the second dG within a GGG sequence. Substrates A-p27 and A-p28 (series-A) are control substrates without a PhIP adduct. The corresponding 3′ complimentary 27- and 28-mer sequences, p27 and p28, were used as extension primers. The template-primer complexes, C-p27 and C-p28, were used to monitor the nucleotide insertions into the site opposite dG-C8-PhIP and the extension reactions from the 3′-dC opposite dG-C8-PhIP, respectively.

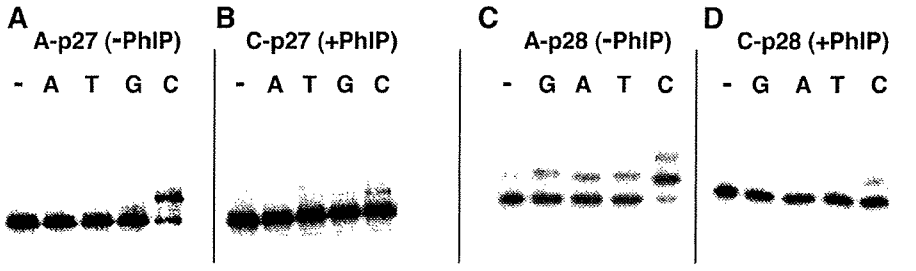

FIGURE 5. **Translesional DNA synthesis by pol η using substrates C-p27 and C-p28.** Control reactions were performed using substrates without the PhIP adduct, A-p27 (*A*) and A-p28 (*C*). An insertion reaction was performed with substrate C-p27 (*B*) and an extension reaction with substrate C-p28 (*D*). A single dNTP (G, A, T, C) was added into the reaction mixture as indicated by *G, A, T,* and *C above* each lane. The lanes indicated by – are controls without any nucleotides. Concentrations of pol η and each dNTP were 1.9 nM and 100 μM, respectively.

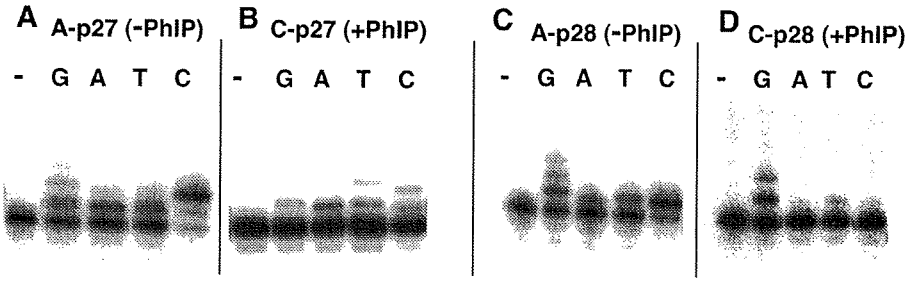

FIGURE 6. **Translesional DNA synthesis by pol κ using substrates C-p27 and C-p28.** Control reactions were performed using substrates without the PhIP adduct, A-p27 (*A*) and A-p28 (*C*). An insertion reaction was performed with substrate C-p27 (*B*) and an extension reaction with substrate C-p28 (*D*). A single dNTP (G, A, T, C) was added into the reaction mixture as indicated by *G*, *A*, *T*, and *C above* each lane. The lanes indicated by − are controls without any nucleotides. The concentrations of pol κ were 250 (*A* and *C*), 500 (*B*), and 1000 nM (*D*), respectively. The concentration of each dNTP was 100 μM.

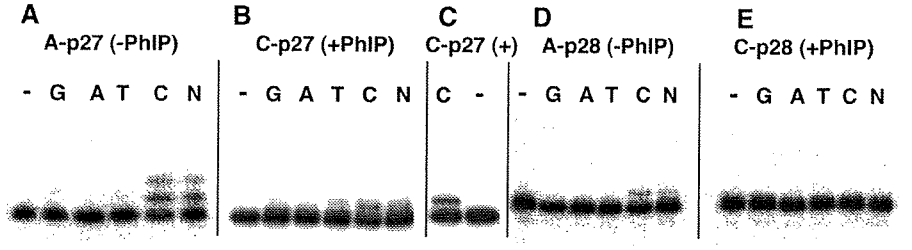

FIGURE 7. **Translesional DNA synthesis by REV1 using substrates C-p27 and C-p28.** Control reactions were performed using substrates without the PhIP adduct, A-p27 (*A*) and A-p28 (*D*). Insertion reactions were performed with substrate C-p27 (*B* and *C*) and an extension reaction with substrate C-p28 (*E*). A single dNTP (G, A, T, and C) or a mixture of each was added into the reaction mixture as indicated by *G*, *A*, *T*, *C*, and *N above* each lane. The lanes indicated by − are controls without any nucleotides. The concentrations of REV1 were 5.2 (*A* and *D*) and 26 nM (*B*, *C*, and *E*), respectively. The concentrations of each dNTP were 100 μM (*A*, *B*, *D*, and *E*) and 320 μM (*C*), respectively. The *N* mixture contained each dNTP at a concentration of 25 μM.

We next examined translesional DNA synthesis beyond the PhIP adduct using a truncated form of human DNA polymerase κ containing the N-terminal 559 amino acids. One or two dCs were inserted opposite the dG-C8-PhIP adduct by this polymerase, and misinsertions of three other nucleotides were also observed to a certain extent (Fig. 6*B*). pol κ incorporated two dCs and misincorporated dG, dA, and dT into the A-p27 substrate without the PhIP adduct at a low efficiency (Fig. 6*A*). Misincorporations of dG, dA, and dT into the A-p28 substrate without the adduct were also observed (Fig. 6*C*). In the case of the extension reaction from 3′-dC opposite the dG-PhIP adduct, pol κ also incorporated dC and misincorporated dT into the C-p28 substrate at low efficiency (Fig. 6*D*). Interestingly, one- and two-base incorporations of dG into the substrate C-p28 by pol κ dominated the incorporation of a dC (Fig. 6*D*). In the extension reaction with pol κ in the presence of all four dNTPs, fragments of 29 and 30 nucleotides were observed as major products, and a small amount of the 31-nucleotide fragment was observed (see supplemental Fig. S5, *lane 6*). Full-length products of 32 nucleotides were observed only when an excess amount of pol κ was present (data not shown). This poor extension activity of pol κ after adding two nucleotides was probably caused by the shortness (~4 nucleotides) of the 5′ region to the lesion in the template oligonucleotide. Extension with pol κ, pol η, and pol δ from the mismatched primers, where the 3′-terminal nucleotide of the p28 primer, dC, was substituted with another nucleotide, could not be observed (data not shown). REV1 inserted a dC opposite the PhIP adduct at a higher efficiency compared with pol κ and pol η (Fig. 7, *B* and *C*). REV1 was, however, unable to catalyze the extension reaction from the dC opposite the PhIP adduct in C-p28 (Fig. 7*E* and supplemental Fig. S5, *lane 5*). REV1 incorporated only dC nucleotides into A-p27 and A-p28 substrates without the adduct (Fig. 7, *A* and *D*). Neither nucleotide insertion nor extension reactions for the templates containing the PhIP adduct were detected using human pol ι (data not shown).

Kinetic Analyses of Translesional DNA Synthesis by pol κ and REV1—To evaluate translesional DNA synthesis beyond the dG-C8-PhIP adduct in further detail, additional quantitative analyses for pol κ and REV1 were performed. Insertion reactions catalyzed by pol κ for dC (Fig. 8, *B*, *lanes 2–5*, and *C*, *closed diamonds*) and dG (Fig. 8, *B*, *lanes 6–9*, and *C*, *closed triangles*) into substrate C-p28 were analyzed in the same way. Kinetic parameters for pol κ were determined using steady-state kinetic assays (Table 2). The catalytic efficiency (k_{cat}/K_m) of dC insertion into C-p28 (0.039 min^{-1} mM^{-1}) was found to be 4-fold greater than that into C-p27 (0.011 min^{-1} mM^{-1}). These results indicate that pol κ catalyzes the extension reaction from the 3′-terminal of dC opposite the dG-C8-PhIP with a higher efficiency than the insertion reaction opposite the adduct. The k_{cat}/K_m values of the dC insertion opposite the adduct were roughly 4 orders of magnitude less than those into counterparts without the adduct (see Table 2). The k_{cat}/K_m value of the dG incorporation into C-p28 was slightly higher than that of dC, and more than 8-fold higher than that of dG into C-p27 (see Table 2). This result indicates that pol κ skipped over the dG site just 5′ of dG-C8-PhIP on the template and incorporated dG opposite dC on the template strand of substrate C-p28 with a high efficiency. The k_{cat}/K_m values of the dC incorporation into D-p27 (0.19 min^{-1} mM^{-1}) were over 4-fold greater than into C-p28 (0.039 min^{-1} mM^{-1}) and over 8-fold higher than that of dG into B-p29 (0.023) (see supplemental Table S1). These data indicate that the efficiencies of the extension reaction by pol κ are the highest for template p32D containing the PhIP adduct in the third G of the triple G run, next for template p32C containing the PhIP/adduct in the second G, and lowest for template p32B containing the PhIP adduct in the first G.

Even at higher concentrations of dNTPs, extension reactions catalyzed by REV1 for substrate C-p28 could not be monitored (Table 3, Fig. 7*E*). The k_{cat}/K_m value of the dC incorporation by REV1 into substrate C-p27 was more than 2,000 times greater than that by pol k, and 1/44 of the values for counterparts with-

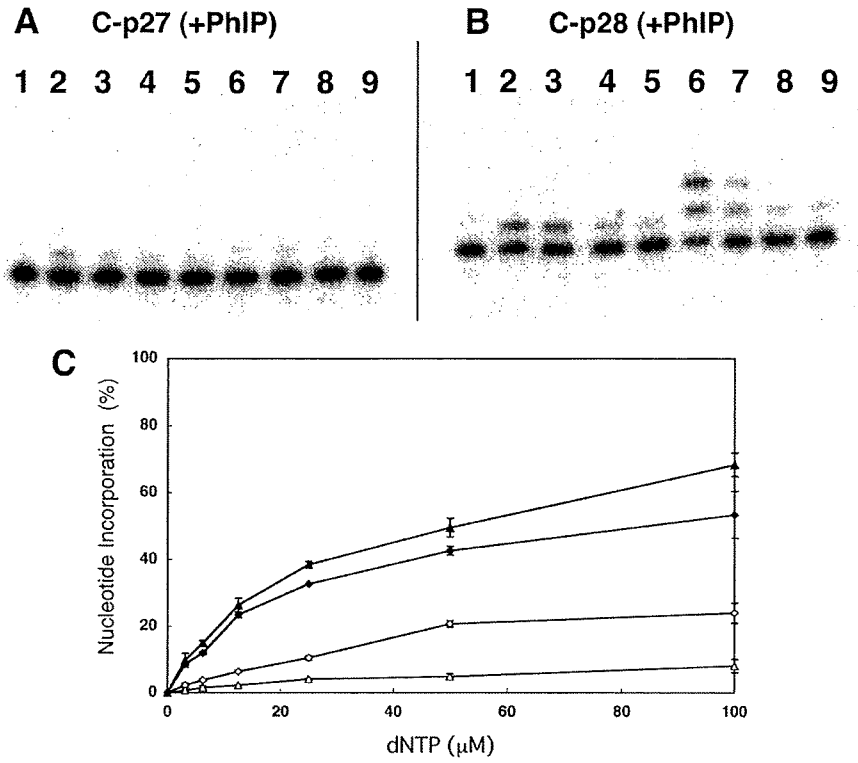

FIGURE 8. **Translesional DNA synthesis by pol κ.** Nucleotide incorporation by pol κ for substrates C-p27 (*A*) and C-p28 (*B*). Either dCTP (*lanes 2-5*) or dGTP (*lanes 6-9*) was added into the reaction mixture. *Lane 1* indicates a control without any nucleotides. The concentration of pol κ was 910 nM. The concentrations of dCTP or dGTP, respectively, were 25 (*lanes 2* and *6*), 12.5 (*lanes 3* and *7*), 6.25 (*lanes 4* and *8*), and 3.13 μM (*lanes 5* and *9*). *C*, incorporation efficiencies of dCTP and dGTP into substrate C-p27 and C-p28. Incorporations of dCTP into C-p27, dGTP into C-p27, dCTP into C-p28, and dGTP into C-p28 are indicated by *open diamonds*, *open triangles*, *closed diamonds*, and *closed triangles*, respectively. Each data point represents the mean of two separate experiments. The *error bars* represent residuals.

TABLE 2
k_{cat}/K_m values for pol κ

Substrate	K_m	k_{cat}	k_{cat}/K_m
	μM	$\times 10^{-3}$ min^{-1}	min^{-1} mM^{-1}
C-p27			
dCTP	70	0.76	0.011
dGTP	47	0.24	0.0050
C-p28			
dCTP	8.0	0.32	0.039
dGTP	11	0.48	0.042
A-p27			
dCTP	0.035	4.4	130
dGTP	0.26	1.3	5.0
A-p28			
dCTP	0.027	3.7	140
dGTP	2.1	8.8	4.1

TABLE 3
k_{cat}/K_m values for dCTP-insertion by REV1

Substrate	K_m	k_{cat}	k_{cat}/K_m
	μM	$\times 10^{-3}$ min^{-1}	min^{-1} mM^{-1}
C-p27	12	320	27
C-p28	ND[a]	ND	ND
A-p27	0.36	390	1100

[a] ND, not detectable.

out the adduct (Table 3). The k_{cat}/K_m values of the dC insertion by REV1 into three substrates, B-p28, C-p27 and D-p26, were 39, 27, and 73 min^{-1} mM^{-1}, respectively. Thus, the insertion reaction catalyzed by REV1 among the three templates was the most efficient for template p32D containing the PhIP adduct at the third G, similar to the extension reaction by pol κ.

DISCUSSION

In Vitro TLS Analysis Reconstituting PhIP-induced Mutations—HCAs are food-borne carcinogens produced when cooking meat (1, 9, 33). The most significant aspect of these molecules is that they exist normally in cooked food and are thus ubiquitous carcinogens (32). The mutagenicity and carcinogenicity of HCAs are mainly attributed to C8- and N2-dG adducts (9). Both excision repair and translesional DNA synthesis play critical roles in the mutagenesis steps induced by HCAs. However, despite the importance of HCAs as common environmental mutagens, there have been very few previous reports regarding the stalling of DNA polymerases and TLS caused by the DNA adducts they form. This is mainly because of the difficulty in preparing template DNA with introduced HCA adducts at specific sites. Choi *et al.* (34) have recently undertaken a biochemical study of TLS at adducts of the HCA 2-amino-3-methylimidazo[4,5-*f*]quinoline (IQ) using purified human polymerases. In our current study of TLS, we describe our findings for adducts of PhIP, the most abundant HCA in cooked foods (4).

A rat colon cancer model induced by PhIP shows profiles of cancer development similar to the multistep model of colon carcinogenesis in humans (35). In this rat model, *p53* and K-*ras* mutations are rarely observed, whereas mutations in *Apc* and its downstream gene *β-catenin* have been frequently observed (21, 36–38). Hence, mutations in *Apc* or *β-catenin* have been speculated to play a critical role in PhIP-induced colon carcinogenesis. Five mutations in the *Apc* gene were previously detected in four of eight PhIP-induced rat colon tumors, and all of these mutations involved a single guanine deletion in the 5′-GGGA-3′ sequence (21). This characteristic mutation induced by PhIP, 5′-GGGA-3′ to 5′-GGA-3′, was also observed in other *in vivo* mutation analyses using transgenic animals harboring introduced reporter genes, such as *lacI* (18–20). Hence, the 5′-TCCGGGAAC-3′ sequence corresponding to a mutation hot spot within the rat *Apc* gene, which we utilized to introduce the PhIP adduct and employed as the template for *in vitro* DNA synthesis analyses, could be a suitable model for revealing the molecular mechanisms associated with PhIP-induced mutations.

As discussed later, our results indicate a possible molecular mechanism for the 5′-GGGA-3′ to 5′-GGA-3′ mutation induced by PhIP.

DNA Polymerases Involved in TLS through the dG-PhIP Adduct—TLS through many DNA lesions requires the action of two different polymerases, an "inserter" and an "extender," the former to perform nucleotide insertions opposite the lesion site and the latter for subsequent extensions (39). The catalytic efficiency of the dCTP-insertion reaction opposite the dG-PhIP adduct by REV1 was found to be more than 2,000-fold greater than that by pol κ (see Tables 2 and 3). This result strongly suggests that REV1 functions *in vivo* as an inserter polymerase for TLS through the dG-PhIP adduct. This insertion step by REV1 is also error free. REV1 has been reported previously to insert dCTP opposite abasic sites and various N2-dG adducts (26, 39–41). However, our current study is the first to show that REV1 inserts dCTP opposite a large size C8-dG adduct. We used a shorter (C-terminal deleted) form of pol κ in our current experiments and an intact pol κ may be more effective for this insertion reaction. As for pol η, a detailed kinetic analysis was not performed. Hence, the possibility cannot be excluded that pol κ and pol η also function as inserter polymerases.

In addition to the Y-family DNA polymerases, DNA polymerase ζ (pol ζ), belonging to the B-family DNA polymerases, is considered to be involved in TLS through various lesions as an extender DNA polymerase (39, 42, 43). We have not carried out a primer extension assay with pol ζ and thus the possibility cannot be completely excluded by our current data that pol ζ functions *in vivo* as an extender polymerase for TLS through the dG-PhIP adduct. In our present study, we provide evidence that pol κ can extend from dC opposite the dG-C8-PhIP adduct *in vitro*. It is, therefore, possible that pol κ, at least partially, functions as an extender polymerase *in vivo* for TLS through the dG-PhIP adduct. Further study about cooperation between two or more DNA polymerases, including pol ζ, is necessary to verify which DNA polymerases are involved in the bypass synthesis through the PhIP lesion.

The catalytic efficiency of pol κ for a dGTP insertion into substrate C-p28 was a little higher than that for dCTP insertions (see Table 2 and Fig. 6*D*). The former generates a single guanine deletion, and the latter is an error-free extension. Consequently, our data suggest that the extension reaction with pol κ from the nucleotide opposite the dG-C8-PhIP adduct causes frequent single-guanine deletions from the GGG stretch. It has been reported that one characteristic feature of pol κ homologs, from bacteria to humans, is their propensity to generate single-base deletions (44–47). The crystal structure of Dpo4, a thermophilic archaea homolog of pol κ, in ternary complexes with DNA and an incoming nucleotide supports the model that a single base deletion by pol κ is generated through a misaligned intermediate complex where the template dG forms an extrahelical looped out structure and the incoming dGTP skips this extrahelical base and pairs with the next template base dC (48) (see supplemental Fig. S6). It is reasonable to speculate therefore that, in the case of TLS through dG-C8-PhIP, mammalian pol κ generates the single guanine deletion via a similar intermediate where the PhIP-adducted dG is looped out and template-primer slippage occurs. However, further analyses for determining whether the one-base skipping of pol κ beyond the lesion observed by us is dependent on the nucleotide placed 5′ to the lesion or not, are necessary to clarify the detailed molecular mechanism underlying one base skipping of pol κ.

Molecular Mechanisms Underlying Mutation Induction by PhIP—We have demonstrated herein by *in vitro* DNA synthesis analyses using oligonucleotide templates containing dG-PhIP that: 1) replicative DNA polymerases stall at the PhIP adduct and cannot perform translesional DNA synthesis beyond this point; 2) REV1 inserts a dC opposite the dG-PhIP with a much higher efficiency than other TLS polymerases, including pol κ and pol η; and 3) pol κ has a potential ability to catalyze an extension reaction from the 5′-dC opposite the adduct and often skips over one dG in the template during this extension step. A working model for the induction of mutations at the PhIP adducts based on the results shown in the present study is illustrated in supplemental Fig. S6. This model could be adopted for other sequences containing a G repeat stretch longer than GGG.

REFERENCES

1. Nagao, M. (2000) in *Food Borne Carcinogens: Heterocyclic Amines* (Nagao, M., and Sugimura, T., eds) pp. 163–196, John Wiley & Sons Ltd., Chichester, UK
2. Schut, H. A., and Snyderwine, E. G. (1999) *Carcinogenesis* **20,** 353–368
3. Felton, J. S., Knize, M. G., Shen, N. H., Lewis, P. R., Andresen, B. D., Happe, J., and Hatch, F. T. (1986) *Carcinogenesis* **7,** 1081–1086
4. Felton, J. S., Jagerstad, M., Knize, M. G., Skog, K., and Wakabayashi, K. (2000) in *Food Borne Carcinogens: Heterocyclic Amines* (Nagao, M., and Sugimura, T., eds) pp. 31–71, John Wiley & Sons Ltd., Chichester, UK
5. Holme, J. A., Wallin, H., Brunborg, G., Søderlund, E. J., Hongslo, J. K., and Alexander, J. (1989) *Carcinogenesis* **10,** 1389–1396
6. Felton, J. S., and Knize, M. G. (1991) *Mutat. Res.* **259,** 205–217
7. Ohgaki, H., Takayama, S., and Sugimura, T. (1991) *Mutat. Res.* **259,** 399–410
8. Ito, N., Hasegawa, R., Sano, M., Tamano, S., Esumi, H., Takayama, S., and Sugimura, T. (1991) *Carcinogenesis* **12,** 1503–1506
9. Sugimura, T., Wakabayashi, K., Nakagama, H., and Nagao, M. (2004) *Cancer Sci.* **95,** 290–299
10. Imaida, K., Hagiwara, A., Yada, H., Masui, T., Hasegawa, R., Hirose, M., Sugimura, T., Ito, N., and Shirai, T. (1996) *Jpn. J. Cancer Res.* **87,** 1116–1120
11. Frandsen, H., Grivas, S., Andersson, R., Dragsted, L., and Larsen, J. C. (1992) *Carcinogenesis* **13,** 629–635
12. Lin, D., Kaderlik, K. R., Turesky, R. J., Miller, D. W., Lay, J. O., Jr., and Kadlubar, F. F. (1992) *Chem. Res. Toxicol.* **5,** 691–697
13. Snyderwine, E. G., Davis, C. D., Nouso, K., Roller, P. P., and Schut, H. A. (1993) *Carcinogenesis* **14,** 1389–1395
14. Schut, H. A., and Herzog, C. R. (1992) *Cancer Lett.* **67,** 117–124
15. Endo, H., Schut, H. A., and Snyderwine, E. G. (1994) *Cancer Res.* **54,** 3745–3751
16. Morgenthaler, P. M., and Holzhäuser, D. (1995) *Carcinogenesis* **16,** 713–718
17. Yadollahi-Farsani, M., Gooderham, N. J., Davies, D. S., and Boobis, A. R. (1996) *Carcinogenesis* **17,** 617–624
18. Okonogi, H., Stuart, G. R., Okochi, E., Ushijima, T., Sugimura, T., Glickman, B. W., and Nagao, M. (1997) *Mutat. Res.* **395,** 93–99
19. Lynch, A. M., Gooderham, N. J., Davies, D. S., and Boobis, A. R. (1998) *Mutagenesis* **13,** 601–605
20. Okochi, E., Watanabe, N., Shimada, Y., Takahashi, S., Wakazono, K., Shirai, T., Sugimura, T., Nagao, M., and Ushijima, T. (1999) *Carcinogenesis* **20,** 1933–1988
21. Kakiuchi, H., Watanabe, M., Ushijima, T., Toyota, M., Imai, K., Weisburger, J. H., Sugimura, T., and Nagao, M. (1995) *Proc. Natl. Acad. Sci.*

U.S.A. **92,** 910–914
22. Takamura-Enya, T., Ishikawa, S., Mochizuki, M., and Wakabayashi, K. (2006) *Chem. Res. Toxicol.* **19,** 770–778
23. Masuda, Y., Suzuki, M., Piao J., Gu, Y., Tsurimoto, T., and Kamiya, K. (2007) *Nucleic Acids Res.* **35,** 6904–6916
24. Masutani, C., Kusumoto, R., Iwai, S., and Hanaoka, F. (2000) *EMBO J.* **19,** 3100–3109
25. Niimi, N., Sassa, A., Katafuchi, A., Grúz, P., Fujimoto, H., Bonala, R. R., Johnson, F., Ohta, T., and Nohmi, T. (2009) *Biochemistry* **48,** 4239–10234246
26. Masuda, Y., and Kamiya, K. (2002) *FEBS Lett.* **520,** 88–92
27. Masuda, Y., Ohmae, M., Masuda, K., and Kamiya, K. (2003) *J. Biol. Chem.* **278,** 12356–12360
28. Sambrook, J., Fritsch, E. F., and Maniatis, T. (1989) *Molecular Cloning: A Laboratory Manual,* 2nd Ed., Cold Spring Harbor Laboratory, Cold Spring Harbor, NY
29. Fukuda, H., and Ohtsubo, E. (1997) *Genes Cells* **2,** 735–751
30. Fukuda, H., Katahira, M., Tsuchiya, N., Enokizono, Y., Sugimura, T., Nagao, M., and Nakagama, H. (2002) *Proc. Natl. Acad. Sci. U.S.A.* **99,** 12685–12690
31. Sugiyama, H., and Saito, I. (1996) *J. Am. Chem. Soc.* **118,** 7063–7068
32. Mozzherin, D. J., Shibutani, S., Tan, C. K., Downey, K. M., and Fisher, P. A. (1997) *Proc. Natl. Acad. Sci. U.S.A.* **94,** 6126–6231
33. Sugimura, T., and Adamson, R. H. (2000) in *Food Borne Carcinogens: Heterocyclic Amines* (Nagao, M., and Sugimura, T., eds) pp. 1–4, John Wiley & Sons Ltd., Chichester, UK
34. Choi, J. Y., Stover, J. S., Angel, K. C., Chowdhury, G., Rizzo, C. J., and Guengerich, F. P. (2006) *J. Biol. Chem.* **281,** 25297–25306
35. Nakagama, H., Ochiai, M., Ubagai, T., Tajima, R., Fujiwara, K., Sugimura, T., and Nagao, M. (2002) *Mutat. Res.* **506–507,** 137–144
36. Nagao, M. (1999) *Mutat. Res.* **431,** 3–12
37. Nagao, M., Ushijima, T., Toyota, M., Inoue, R., and Sugimura, T. (1997) *Mutat. Res.* **376,** 161–167
38. Dashwood, R. H., Suzui, M., Nakagama, H., Sugimura, T., and Nagao, M. (1998) *Cancer Res.* **58,** 1127–1129
39. Prakash, S., Johnson, R. E., and Prakash, L. (2005) *Annu. Rev. Biochem.* **74,** 317–353
40. Nelson, J. R., Lawrence, C. W., and Hinkle, D. C. (1996) *Nature* **382,** 729–731
41. Haracska, L., Prakash, S., and Prakash, L. (2002) *J. Biol. Chem.* **277,** 15546–15551
42. Johnson, R. E., Washington, M. T., Haracska, L., Prakash, S., and Prakash, L. (2000) *Nature* **406,** 1015–1019
43. Haracska, L., Unk, I., Johnson, R. E., Johansson, E., Burgers, P. M., Prakash, S., and Prakash, L. (2001) *Genes Dev.* **15,** 945–954
44. Kim, S. R., Maenhaut-Michel, G., Yamada, M., Yamamoto, Y., Matsui, K., Sofuni, T., Nohmi, T., and Ohmori, H. (1997) *Proc. Natl. Acad. Sci. U.S.A.* **94,** 13792–13797
45. Kobayashi, S., Valentine, M. R., Pham, P., O'Donnell, M., and Goodman, M. F. (2002) *J. Biol. Chem.* **277,** 34198–34207
46. Ogi, T., Kato, T., Jr., Kato, T., and Ohmori, H. (1999) *Genes Cells* **4,** 607–618
47. Ohashi, E., Bebenek, K., Matsuda, T., Feaver, W. J., Gerlach, V. L., Friedberg, E. C., Ohmori, H., and Kunkel, T. A. (2000) *J. Biol. Chem.* **275,** 39678–39684
48. Ling, H., Boudsocq, F., Woodgate, R., and Yang, W. (2001) *Cell* **107,** 91–102

FEBS Letters 583 (2009) 2710–2714

FEBS Letters

journal homepage: www.FEBSLetters.org

Mdmx enhances p53 ubiquitination by altering the substrate preference of the Mdm2 ubiquitin ligase

Koji Okamoto [a,b,c], Yoichi Taya [b,c,1], Hitoshi Nakagama [a,*]

[a] National Cancer Center Research Institute, Early Oncogenesis Research Project, 5-1-1 Tsukiji, Chuo-ku, Tokyo 104-0045, Japan
[b] National Cancer Center Research Institute, Radiobiology Division, 5-1-1 Tsukiji, Chuo-ku, Tokyo 104-0045, Japan
[c] SORST, Japan Science and Technology Corporation, Japan

ARTICLE INFO

Article history:
Received 11 May 2009
Revised 26 June 2009
Accepted 13 July 2009
Available online 18 July 2009

Edited by Noboru Mizushima

Keywords:
Mdmx
Mdm2
p53
Ubiquitination

ABSTRACT

***mdm2* and *mdmx* oncogenes play essential yet non-redundant roles in synergistic inactivation of the tumor suppressor, p53. While Mdm2 inhibits p53 activity mainly by augmenting its ubiquitination, the functional role of Mdmx on p53 ubiquitination remains obscure. In transfected H1299 cells, Mdmx augmented Mdm2-mediated ubiquitination of p53. In in vitro ubiquitination assays, the Mdmx/Mdm2 heteromeric complex, in comparison to the Mdm2 homomer, showed enhanced ubiquitinase activity toward p53 and the reduced auto-ubiquitination of Mdm2. Alteration of the substrate specificity via binding to Mdmx may contribute to efficient ubiquitination and inactivation of p53 by Mdm2.**

Structured summary:
MINT-7219995: *P53* (uniprotkb:P04637) *physically interacts* (MI:0914) with *Ubiquitin* (uniprotkb:P62988) by *anti bait coimmunoprecipitation* (MI:0006)
MINT-7220023: *Ubiquitin* (uniprotkb:P62988) *physically interacts* (MI:0914) with *P53* (uniprotkb:P04637) by *pull down* (MI:0096)

1. Introduction

The p53 tumor suppressor protein plays a central role in preventing tumorigenesis. p53 functions as a sequence-specific transcriptional factor [1,2], and activated p53 exerts its function as a tumor suppressor by inducing numerous target genes [3–6]. In most cancer cells, its activity is lost via alteration of its gene or via other cellular events that inactivate p53 [7–9].

Mdm2 and Mdmx function as two major players in the suppression of p53 activity [10]. Accumulating reports indicate that the major function of Mdm2 in suppressing p53 is attributed to Mdm2-dependent p53 ubiquitination, which triggers proteasomal degradation or nuclear export of p53 [11], although it has been reported that Mdm2 inactivates p53 by other mechanisms [12–15]. Mdm2 possesses a RING finger domain, a protein–protein interaction motif that is found in many eukaryotic proteins and often possesses E3 ubiquitin ligase activity [16]. Indeed, Mdm2 functions as an E3 ubiquitin ligase, and the RING domain of Mdm2 is essential for its ubiquitin ligase activity toward p53 and Mdm2 itself [17–19].

Mdmx shares an extensive structural homology with Mdm2, and forms a heterodimer complex with Mdm2 through their RING finger domains [20,21], yet Mdmx in itself lacks the robust activity of an E3 ubiquitin ligase [22]. Thus, both genetic and biochemical evidence indicates that Mdmx and Mdm2 perform distinct yet co-operative functions in p53 inactivation.

Recent reports suggest that Mdmx may inactivate p53 by augmenting Mdm2-mediated ubiquitination of p53 [23–25]. However, precise mechanism by which Mdmx stimulates p53 ubiquitination by Mdm2 is not yet known.

In this paper, we demonstrated that wild-type Mdmx is capable of enhancing Mdm2-mediated p53 ubiquitination in vivo. Further, the in vitro study using purified Mdm2 or the Mdm2/Mdmx complex revealed that, when complexed with Mdmx, the extent of p53 ubiquitination by Mdm2 was enhanced while poly-ubiquitination of Mdm2 was significantly decreased. We propose that the effect of Mdmx on the preference of the substrate of the Mdm2 ubiquitin ligase plays an important role in effective ubiquitination of p53.

* Corresponding author.
E-mail address: hnakagam@ncc.go.jp (H. Nakagama).
[1] Present address: Cancer Science Institute of Singapore, National University of Singapore, Singapore 117456, Singapore.

0014-5793/$36.00 © 2009 Federation of European Biochemical Societies. Published by Elsevier B.V. All rights reserved.
doi:10.1016/j.febslet.2009.07.021

2. Materials and methods

2.1. DNA transfection

In DNA transfection experiments using H1299 cells, 2 μg of DNA and 4 μl of Lipofectamine 2000 reagent (Invitrogen) were introduced per 2.0×10^5 cells according to manufacturer's protocol. Cells were then incubated for 20 h before harvesting.

2.2. In vivo ubiquitination assay

For detection of p53 conjugated with endogenous ubiquitin, in vivo ubiquitination assays were performed as previously described [26] with some modifications. Transfected H1299 cells were lysed in SDS lysis buffer (50 mM Tris, pH 7.5, 100 mM NaCl, 1% SDS) supplemented with 1 mM DTT and protease inhibitor cocktail (PI) [27], boiled for 10 min, and diluted with ×4 volumes of dilution buffer (50 mM Tris, pH 7.5, 100 mM NaCl, 1.25% Triton X-100) supplemented with DTT and PI. After sonication of the lysates, p53 was immunoprecipitated with anti-p53 antibody (DO-1). Subsequently the immunoprecipitates were washed three times with 200-NP buffer [27], and analyzed by Western blotting with DO-1 and anti-ubiquitin antibody (FK2, MBL).

For detection of p53 conjugated with transfected $(His)_6$-ubiquitin, transfected H1299 cells were lysed in urea lysis buffer (100 mM NaH2PO4, 10 mM Tris–HCl, pH 8.0, 500 mM NaCl, 10% glycerol, 0.1% Triton X-100, 10 mM imidazole) supplemented with 10 mM β-mercaptoethanol, PI, 5 mM Iodoacetamide, and 1 mg/ml NEM. Proteins conjugated with His-tagged ubiquitin were purified as described before [28], and analyzed by Western blot analysis.

2.3. Protein expression and purification

Flag-tagged Human Mdm2 (Flag-Mdm2) or Human Mdmx RNA was transcribed from the corresponding cDNA using the Wheat Germ Expression Kit (Cell Free Science, Japan). Subsequently, the Flag-Mdm2 RNA alone or in combination with an excess amount of the Mdmx RNA was used for in vitro translation with wheat germ lysate (Cell Free Science) according to the manufacturer's instructions. Flag-Mdm2 or the Flag-Mdm2/Mdmx complex was then purified on agarose conjugated with anti-Flag antibody.

2.4. In vitro ubiquitination assay

In vitro ubiquitination assays were performed as previously described with some modifications [29]. Approximately 100 ng of Flag-Mdm2 or the Flag-Mdm2/Mdmx complex were mixed with the following purified components; 8 ng of GST-p53, 10 ng of E1 (Boston Biochem), 80 ng of E2 (UbcH5b, Boston Biochem), 3 μg of His-ubiquitin (Calbiochem), or methylated ubiquitin (Boston Biochem). In experiments shown in Fig. 4D, ^{125}I-ubiquitin (Perkin–Elmer) was included in the reaction mixture. These components were incubated in a reaction buffer (40 mM Tris–HCl, pH 7.5, 5 mM $MgCl_2$, 10 mM NaCl) in the presence of 2 mM Mg–ATP at 37 °C for the indicated times. After the reactions were terminated by adding SDS sample buffer, ubiquitinated proteins were separated in SDS–PAGE gels and detected by Western blot analyses or autoradiography.

3. Results

3.1. Wild-type Mdmx was capable of enhancing p53 ubiquitination in the presence of Mdm2 in vivo

Recently, we demonstrated that the non-phosphorylatable, active form of Mdmx augments p53 ubiquitination mediated by wild-type Mdm2 in transfected H1299 cells [30]. In order to determine whether wild-type Mdmx cooperates with Mdm2 to induce ubiquitination of p53 as well, wild-type Mdmx (Mdmx-wt) or the non-phosphorylated form of Mdmx (Mdmx-3A) was transfected together with Mdm2 into H1299 cells, and conjugation of p53 with endogenous ubiquitin was examined by Western blot analyses (Fig. 1). As expected from previous observation [30], Mdmx-3A, which is resistant to Mdm2-mediated ubiquitination and degradation, was expressed at higher levels than wild-type Mdmx (Fig. 1, lanes 2 and 3). p53 ubiquitination induced by Mdm2 was enhanced in the presence of co-transfected wild-type Mdmx (Fig. 1, lanes 5 and 8), indicating that wild-type Mdmx is capable of stimulating Mdm2-mediated ubiquitination of p53,

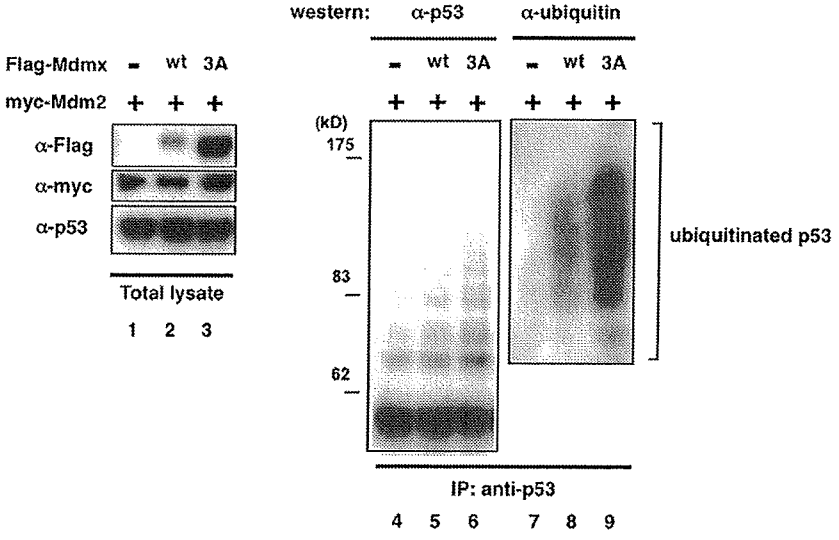

Fig. 1. Mdmx cooperates with Mdm2 to induce p53 ubiquitination. HA-p53 (0.15 mg) and either 0.4 mg of the control vector, wild-type Flag-Mdmx, or the Flag-Mdmx-3A mutant were transfected into H1299 cells in the presence of 0.2 mg of Myc-Mdm2. The total amount of transfected DNA was adjusted to 2 μg with pBluescript plasmid (Stratagene). Twenty hours after transfection, lysates prepared under denaturing conditions were used for immunoprecipitaiton with anti-p53 (DO-1) antibody. The immunoprecipitates were then used for Western blot analyses with DO-1 (left panel, and right bottom panel for low exposure) and with anti-ubiquitin antibody (right panel). Amounts of immunoprecipitates used for Western were normalized such that an equal amount of non-ubiquitinated p53 was loaded in each lane.

although the extent of the stimulation is less than that induced by the non-phosphorylatable mutant (Fig. 1, lanes 6 and 9).

3.2. Mutation at the C-terminal ubiquitinated lysines largely abolished p53 ubiquitination by Mdmx

It has been documented that Mdm2 ubiquitinates p53 at the six C-terminal lysines, the integrity of which are required for its nuclear export [31,32]. We created a mutant p53 in which all six lysines at the C-terminal domain (Fig. S1) were substituted by arginine (p53-K6R), and introduced wild-type p53 or the K6R mutant into H1299 cells together with Mdm2 in the presence or absence of Mdmx-3A. Examination of p53 ubiquitination in vivo revealed that the K6R mutation eliminates a majority of p53 ubiquitination enhanced by Mdmx (Fig. S2), indicating the six lysines were major sites for Mdmx-dependent ubiquitination.

3.3. Association of Mdmx with Mdm2 augments the ability of Mdm2 to ubiquitinate p53 and inhibits poly-ubiquitination of Mdm2 in vitro

In order to determine whether Mdmx enhances Mdm2-dependent ubiquitination of p53 via direct association with Mdm2, we next performed in vitro ubiquitination assays using purified recombinant proteins of Mdm2 or an Mdm2/Mdmx complex (see Section 2). Silver staining of the purified proteins indicated that the co-purified Mdmx formed a complex with Mdm2 at approximately a 1:1 molar ratio (Fig. 2A, right panel).

In order to determine the effect of the association with Mdmx on the activity of E3 ubiquitin ligase of Mdm2, homomeric Mdm2 or the Mdmx/Mdm2 complex was incubated with E1, E2 (UbcH5b), GST-p53, and ubiquitin, and time-course analyses of the ubiquitination of p53 and auto-ubiquitination of Mdm2 were simultaneously performed. The complex formation of Mdm2 with Mdmx-3A or with wild-type Mdmx resulted in an increase of p53 ubiquitination (Fig. 2B and C). In contrast, the Mdmx/Mdm2 complex showed a marked decrease in poly-ubiquitinated forms of Mdm2 in comparison to homomeric Mdm2 (Fig. 2B and C), indicating that the association with Mdmx-3A augments Mdm2-dependent p53 ubiquitination while it inhibits poly-ubiquitination of Mdm2.

3.4. Mdmx inhibits ubiquitination of the Mdm2-containing enzymatic complex

In order to confirm that Mdmx inhibits auto-ubiquitination of Mdm2, in vitro ubiquitination assays of the Mdm2 homomer or the Mdm2/Mdmx complex were performed in the presence of

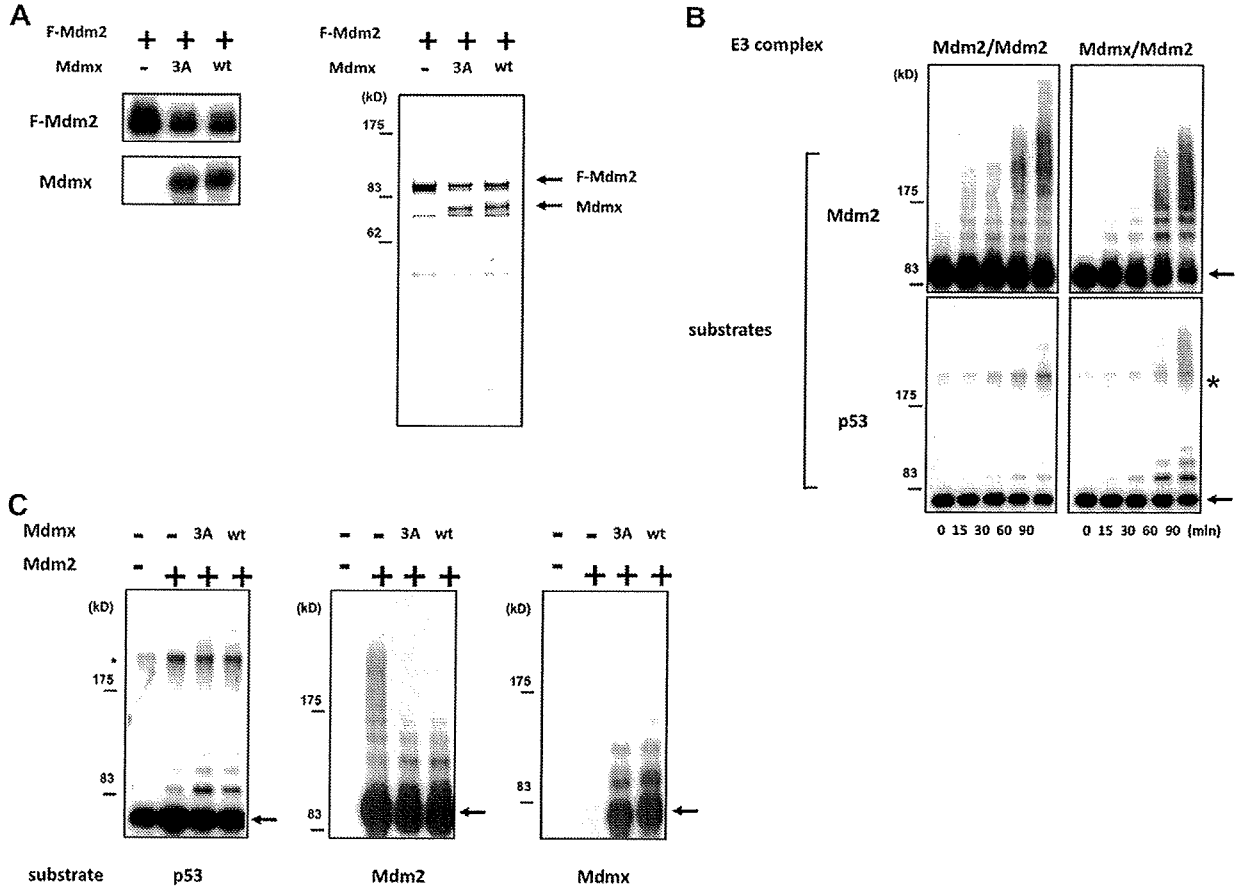

Fig. 2. Association of Mdmx with Mdm2 augments the activity of Mdm2 to ubiquitinate p53 and inhibits auto-ubiquitination of Mdm2 in vitro. (A) Purification of Mdm2 and the Mdm2/Mdmx complex. Flag-tagged Mdm2 was translated alone, or co-translated with Mdmx-3A or wild-type Mdmx in wheat germ lysates, as described in Section 2. The purified proteins were separated by10% SDS–PAGE, and detected by silver staining (right panel), or by Western blotting analyses with anti-Flag antibody (M2) or anti-Mdmx antibody (D-19) (left panel). (B) *In vitro* ubiquitination assays were performed with purified Mdm2 or Mdmx-3A/Mdm2. Ubiquitination reactions were terminated at the indicated times, and the extent of p53 ubiquitination and Mdm2 auto-ubiquitination was evaluated by Western blot analyses with anti-Flag antibody or anti-p53 antibody. The position of non-ubiquitinated substrates is designated by arrows. (C) In vitro ubiquitination assays were performed as described in (B), and the ubiquitination reactions were terminated after 30 min. Ubiquitination of Mdmx, p53, and Mdm2 was evaluated by Western blot analyses.

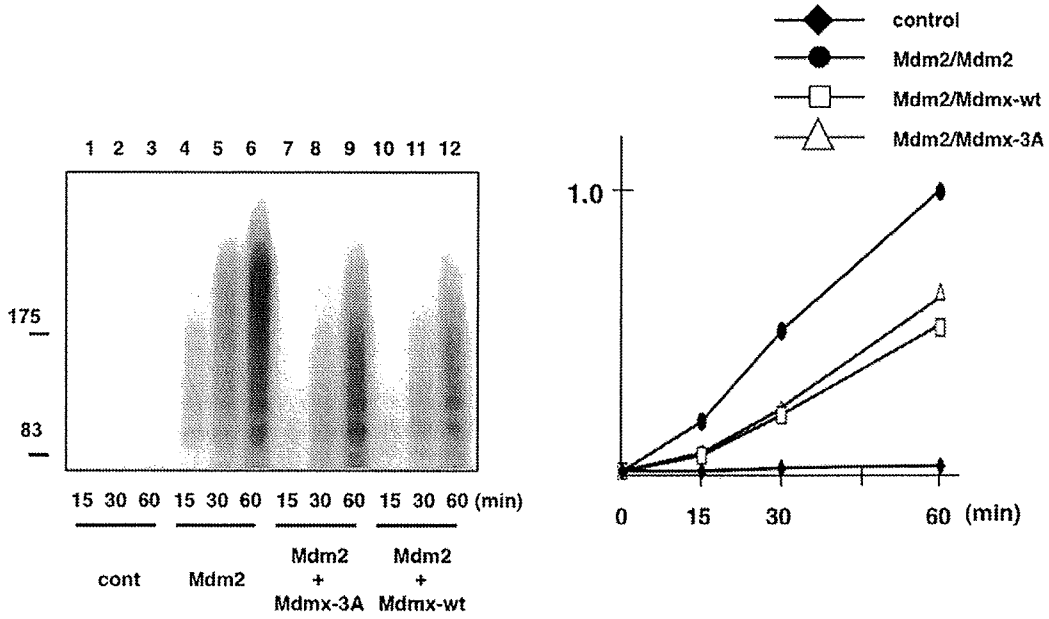

Fig. 3. In vitro ubiquitination reaction was performed as described in Fig. 2C, except that ^{125}I-labeled ubiquitin was included in the reaction. (left panel) Ubiquitinated Mdm2 or Mdm2/Mdmx was separated by 10% SDS–PAGE, and detected by autoradiography. Note that the ladder represents a mixture of ubiqutination of Mdm2 and Mdmx in lanes 7–12 (left panel). Levels of the ubiquitination were quantified and relative levels of ubiquitination were plotted (right panel).

^{125}I-labeled ubiquitin. Quantification of ubiquitin attached to the enzymatic complexes demonstrated that the auto-ubiquitination of the Mdm2 was indeed hindered by the complex formation with either wild-type Mdmx or Mdmx-3A (Fig. 3). Thus, the complex formation of Mdm2 with Mdmx affects the preference for the substrate of the Mdm2 ubiquitin ligase.

3.5. Mdmx stimulates Mdm2-dependent mono-ubiquitination of p53

It has been documented that poly-ubiquitination of p53 induces its degradation, while its mono-ubiquitnation stimulates nuclear export of p53 [33]. Because Mdmx does not significantly contribute to p53 degradation [34], we attempted to determine whether Mdmx stimulates mono-ubiquitination of p53 rather than its poly-ubiquitination. Mdm2 and p53 were introduced into H1299 cells together with His-Ub-K7R, $(His)_6$-tagged mutant ubiquitin which is not capable of forming a ladder of poly-ubiquitination due to arginine substitution in all seven lysine residues [29]. Subsequently, His-Ub-K7R was purified from lysates that were prepared from transfected cells, and p53 conjugated with His-Ub-7KR was detected by Western blot analyses with anti-p53 antibody. The introduction of wild-type Mdmx augmented mono-ubiquitination of p53 (Fig. 4, lane 2), and the Mdmx-3A mutation further enhanced the p53 mono-ubiquitination (Fig. 4, lane 3).

In order to determine whether Mdmx stimulates Mdm2-dependent mono-ubiquitination of p53 in vitro as well as in vivo, methylated ubiquitin was used instead of wild-type ubiquitin in in vitro ubiquitination assays. Indeed, the Mdmx/Mdm2 complex showed a stronger activity for p53 mono-ubiquitination than the homomeric Mdm2 (Fig. S3). Thus, the formation of a complex with Mdmx augments the activity of Mdm2 to mono-ubiquitinate p53.

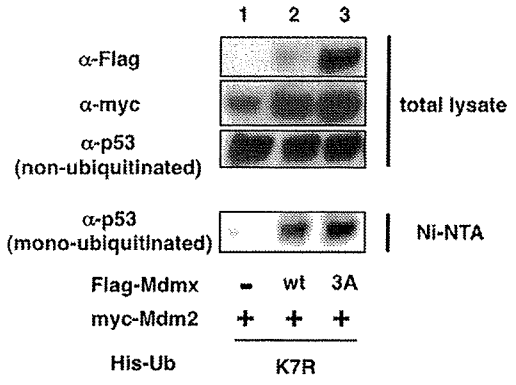

Fig. 4. Mdmx-3A or the control vector was transfected into H1299 cells together with Myc-Mdm2, HA-p53 and the indicated $(His)_6$-tagged ubiquitin K7R mutant. Twenty hours after transfection, cells were lysed with a buffer containing 6 M urea, and normalized lysates that contain equal amounts of non-ubiquitinated p53 were used to purify His-tagged ubiquitin on Ni-NTA agarose (QIAGEN). Ubiquitinated p53 was detected by Western blot analysis with anti-p53 antibody (DO-1).

4. Discussion

In this report, we demonstrated that wild-type Mdmx as well as its non-phosphorylatable mutant cooperates with Mdm2 to stimulate ubiquitination of p53 both in vivo and in vitro. In agreement with our observation, it was reported that Mdmx enhances the activity of Mdm2 as a ubiquitin ligase in vitro [35]. Mdmx complements the catalytic function of mutant Mdm2 proteins that are deficient in the enzymatic activity as a ubiquitin ligase [23–25] and Mdmx/Mdm2 hetero-RING complexes exhibit a greater E3 ligase activity than homomeric Mdm2 [36]. Such effects of Mdmx on Mdm2 should enhance Mdm2-dependent ubiquitination of p53, consistent with the role of Mdmx as an inhibitor of p53.

It was previously reported that Mdmx augments not only auto-ubiquitination of Mdm2 but also the ubiquitin ligase activity of Mdm2 toward p53 [35] in in vitro assays. However, auto-ubiquitination of the Mdm2 ubiquitin ligase negatively affects its activity because poly-ubiquitinated Mdm2 is targeted for proteasome-mediated degradation. Therefore, enhanced ubiquitinase activity of Mdm2 by Mdmx may not be translated into efficient stimulation of p53 ubiquitination if the association of Mdmx to Mdm2 simultaneously leads to stimulation of self-destruction of Mdm2. Our

observation that Mdmx inhibits poly-ubiquitination of Mdm2 while it stimulates p53 ubiquitination may attribute to a mechanism by which Mdmx stimulates Mdm2-dependent p53 ubiquitination without enhanced destruction of Mdm2, thus providing the molecular basis of how Mdmx cooperates with Mdm2 to inhibit p53 activity.

Recently Linke et al. reported the crystal structure of the heterodimer of Mdmx/Mdm2 RING domain, and proposed a model that favors transfer of ubiquitin to Mdmx that does not interact with E2 [37]. This can explain why Mdm2 is not extensively ubiquitinated in the Mdmx/Mdm2 heteromeric complex, thus providing mechanistic basis for reduced ubiquitination of Mdm2 in the Mdmx/Mdm2 complex (Fig. 2). It is noteworthy that, in in vitro ubiquitination assays, the levels of Mdm2 ubiquitination in the homomeric Mdm2 are higher than combined levels of ubiquitination of Mdm2 and Mdmx in the heteromeric complex (Fig. 3). Therefore, it is likely that Mdmx is relatively resistant to ubiquitination by bound Mdm2, unless Mdmx undergoes specific modification such as phosphorylation [27].

It is not clear at this moment how Mdmx stimulates Mdm2-mediated ubiquitination of p53. Mdm2 bound to Mdmx may position its catalytic domain more closer to the C-terminal domain of p53 than homomeric Mdm2, resulting in enhanced p53 ubiquitination. Alternatively, Mdm2 or Mdmx may compete with p53 as a substrate for Mdm2, and relative resistance of Mdmx against ubiquitination by bound Mdm2 may translate into facilitated p53 ubiquitination. Presumably, these two possibilities are not mutually exclusive, and combined effects of Mdmx on Mdm2-mediated ubiquitination may serve to stimulate ubiquitination and inactivation of p53.

Acknowledgements

We thank Aart Jochemsen for helpful suggestions. The His-ubiquitin expression plasmids were kind gifts from Wei Gu. We thank Kenji Kashima and Chihiro Ohtsubo for experimental assistance. This work was supported by a Grant-in-Aid for Scientific Research from the Ministry of Education, Culture, Sports, Science and Technology of Japan (Y.T and K.O.), a Grant-in-Aid for Third Term Comprehensive Control Research for Cancer from the Ministry of Health, Labor and Welfare, Japan (Y.T.), and the Foundation for Promotion of Cancer Research (K.O.).

Appendix A. Supplementary data

Supplementary data associated with this article can be found, in the online version, at doi:10.1016/j.febslet.2009.07.021.

References

[1] Levine, A.J. (1997) P53, the cellular gatekeeper for growth and division. Cell 88, 323–331.
[2] Laptenko, O. and Prives, C. (2006) Transcriptional regulation by p53: one protein, many possibilities. Cell Death Differ. 13, 951–961.
[3] Levine, A.J., Hu, W. and Feng, Z. (2006) The P53 pathway: what questions remain to be explored? Cell Death Differ. 13, 1027–1036.
[4] Oren, M. (2003) Decision making by p53: life, death and cancer. Cell Death Differ. 10, 431–442.
[5] Ko, L.J. and Prives, C. (1996) P53: puzzle and paradigm. Genes Dev. 10, 1054–1072.
[6] Vogelstein, B., Lane, D. and Levine, A.J. (2000) Surfing the p53 network. Nature 408, 307–310.
[7] Lozano, G. and Zambetti, G.P. (2005) What have animal models taught us about the p53 pathway? J. Pathol. 205, 206–220.
[8] Vousden, K.H. and Lu, X. (2002) Live or let die: the cell's response to p53. Nat. Rev. Cancer 2, 594–604.
[9] Olivier, M., Eeles, R., Hollstein, M., Khan, M.A., Harris, C.C. and Hainaut, P. (2002) The IARC TP53 database: new online mutation analysis and recommendations to users. Hum. Mutat. 19, 607–614.
[10] Marine, J.C., Francoz, S., Maetens, M., Wahl, G., Toledo, F. and Lozano, G. (2006) Keeping p53 in check: essential and synergistic functions of Mdm2 and Mdm4. Cell Death Differ. 13, 927–934.
[11] Michael, D. and Oren, M. (2003) The p53-Mdm2 module and the ubiquitin system. Semin. Cancer Biol. 13, 49–58.
[12] Momand, J., Zambetti, G.P., Olson, D.C., George, D. and Levine, A.J. (1992) The mdm-2 oncogene product forms a complex with the p53 protein and inhibits p53-mediated transactivation. Cell 69, 1237–1245.
[13] Oliner, J.D., Pietenpol, J.A., Thiagalingam, S., Gyuris, J., Kinzler, K.W. and Vogelstein, B. (1993) Oncoprotein MDM2 conceals the activation domain of tumour suppressor p53. Nature 362, 857–860.
[14] Ito, A., Lai, C.H., Zhao, X., Saito, S., Hamilton, M.H., Appella, E. and Yao, T.P. (2001) P300/CBP-mediated p53 acetylation is commonly induced by p53-activating agents and inhibited by MDM2. Embo J. 20, 1331–1340.
[15] Kobet, E., Zeng, X., Zhu, Y., Keller, D. and Lu, H. (2000) MDM2 inhibits p300-mediated p53 acetylation and activation by forming a ternary complex with the two proteins. Proc. Natl. Acad. Sci. USA 97, 12547–12552.
[16] Joazeiro, C.A. and Weissman, A.M. (2000) RING finger proteins: mediators of ubiquitin ligase activity. Cell 102, 549–552.
[17] Fang, S., Jensen, J.P., Ludwig, R.L., Vousden, K.H. and Weissman, A.M. (2000) Mdm2 is a RING finger-dependent ubiquitin protein ligase for itself and p53. J. Biol. Chem. 275, 8945–8951.
[18] Honda, R. and Yasuda, H. (2000) Activity of MDM2, a ubiquitin ligase, toward p53 or itself is dependent on the RING finger domain of the ligase. Oncogene 19, 1473–1476.
[19] Honda, R., Tanaka, H. and Yasuda, H. (1997) Oncoprotein MDM2 is a ubiquitin ligase E3 for tumor suppressor p53. FEBS Lett. 420, 25–27.
[20] Tanimura, S., Ohtsuka, S., Mitsui, K., Shirouzu, K., Yoshimura, A. and Ohtsubo, M. (1999) MDM2 interacts with MDMX through their RING finger domains. FEBS Lett. 447, 5–9.
[21] Sharp, D.A., Kratowicz, S.A., Sank, M.J. and George, D.L. (1999) Stabilization of the MDM2 oncoprotein by interaction with the structurally related MDMX protein. J. Biol. Chem. 274, 38189–38196.
[22] Stad, R., Little, N.A., Xirodimas, D.P., Frenk, R., van der Eb, A.J., Lane, D.P., Saville, M.K. and Jochemsen, A.G. (2001) Mdmx stabilizes p53 and Mdm2 via two distinct mechanisms. EMBO Rep. 2, 1029–1034.
[23] Singh, R.K., Iyappan, S. and Scheffner, M. (2007) Hetero-oligomerization with MdmX rescues the ubiquitin/Nedd8 ligase activity of RING finger mutants of Mdm2. J. Biol. Chem. 282, 10901–10907.
[24] Uldrijan, S., Pannekoek, W.J. and Vousden, K.H. (2007) An essential function of the extreme C-terminus of MDM2 can be provided by MDMX. Embo J. 26, 102–112.
[25] Poyurovsky, M.V., Priest, C., Kentsis, A., Borden, K.L., Pan, Z.Q., Pavletich, N. and Prives, C. (2007) The Mdm2 RING domain C-terminus is required for supramolecular assembly and ubiquitin ligase activity. Embo J. 26, 90–101.
[26] Carter, S., Bischof, O., Dejean, A. and Vousden, K.H. (2007) C-terminal modifications regulate MDM2 dissociation and nuclear export of p53. Nat. Cell Biol. 9, 428–435.
[27] Okamoto, K., Kashima, K., Pereg, Y., Ishida, M., Yamazaki, S., Nota, A., Teunisse, A., Migliorini, D., Kitabayashi, I., Marine, J.C., Prives, C., Shiloh, Y., Jochemsen, A.G. and Taya, Y. (2005) DNA damage-induced phosphorylation of MdmX at serine 367 activates p53 by targeting MdmX for Mdm2-dependent degradation. Mol. Cell Biol. 25, 9608–9620.
[28] de Graaf, P., Little, N.A., Ramos, Y.F., Meulmeester, E., Letteboer, S.J. and Jochemsen, A.G. (2003) Hdmx protein stability is regulated by the ubiquitin ligase activity of Mdm2. J. Biol. Chem. 278, 38315–38324.
[29] Li, M., Brooks, C.L., Wu-Baer, F., Chen, D., Baer, R. and Gu, W. (2003) Mono- versus polyubiquitination: differential control of p53 fate by Mdm2. Science 302, 1972–1975.
[30] Ohtsubo, C., Shiokawa, D., Kodama, M., Gaiddon, C., Nakagama, H., Jochemsen, A.G., Taya, Y. and Okamoto, K. (2009) Cytoplasmic tethering is involved in synergistic inhibition of p53 by Mdmx and Mdm2. Cancer Sci.
[31] Gu, J., Nie, L., Wiederschain, D. and Yuan, Z.M. (2001) Identification of p53 sequence elements that are required for MDM2-mediated nuclear export. Mol. Cell Biol. 21, 8533–8546.
[32] Lohrum, M.A., Woods, D.B., Ludwig, R.L., Balint, E. and Vousden, K.H. (2001) C-terminal ubiquitination of p53 contributes to nuclear export. Mol. Cell Biol. 21, 8521–8532.
[33] Shmueli, A. and Oren, M. (2004) Regulation of p53 by Mdm2: fate is in the numbers. Mol. Cell 13, 4–5.
[34] Toledo, F., Krummel, K.A., Lee, C.J., Liu, C.W., Rodewald, L.W., Tang, M. and Wahl, G.M. (2006) A mouse p53 mutant lacking the proline-rich domain rescues Mdm4 deficiency and provides insight into the Mdm2-Mdm4-p53 regulatory network. Cancer Cell 9, 273–285.
[35] Linares, L.K., Hengstermann, A., Ciechanover, A., Muller, S. and Scheffner, M. (2003) HdmX stimulates Hdm2-mediated ubiquitination and degradation of p53. Proc. Natl. Acad. Sci. USA 100, 12009–12014.
[36] Kawai, H., Lopez-Pajares, V., Kim, M.M., Wiederschain, D. and Yuan, Z.M. (2007) RING domain-mediated interaction is a requirement for MDM2's E3 ligase activity. Cancer Res. 67, 6026–6030.
[37] Linke, K., Mace, P.D., Smith, C.A., Vaux, D.L., Silke, J. and Day, C.L. (2008) Structure of the MDM2/MDMX RING domain heterodimer reveals dimerization is required for their ubiquitylation in trans. Cell Death Differ.

Molecular Biology of the Cell
Vol. 20, 2186–2195, April 15, 2009

The Extracellular Signal-regulated Kinase–Mitogen-activated Protein Kinase Pathway Phosphorylates and Targets Cdc25A for SCF$^{\beta\text{-TrCP}}$-dependent Degradation for Cell Cycle Arrest

Michitaka Isoda,* Yoshinori Kanemori,* Nobushige Nakajo,* Sanae Uchida[†‡] Katsumi Yamashita,[†] Hiroyuki Ueno,* and Noriyuki Sagata*[§]

*Department of Biology, Graduate School of Sciences, Kyushu University, Hakozaki 6-10-1, Fukuoka 812-8581, Japan; [†]Division of Life Science, Graduate School of Natural Science and Technology; [‡]Venture Business Laboratory, Center for Innovation, Kanazawa University, Kanazawa 920-1192, Ishikawa, Japan; and [§]CREST, Japan Science and Technology Agency, Nihonbashi, Tokyo 103-0027, Japan

Submitted January 6, 2009; Revised February 18, 2009; Accepted February 18, 2009
Monitoring Editor: Daniel J. Lew

The extracellular signal-regulated kinase (ERK) pathway is generally mitogenic, but, upon strong activation, it causes cell cycle arrest by a not-yet fully understood mechanism. In response to genotoxic stress, Chk1 hyperphosphorylates Cdc25A, a positive cell cycle regulator, and targets it for Skp1/Cullin1/F-box protein (SCF)$^{\beta\text{-TrCP}}$ ubiquitin ligase-dependent degradation, thereby leading to cell cycle arrest. Here, we show that strong ERK activation can also phosphorylate and target Cdc25A for SCF$^{\beta\text{-TrCP}}$-dependent degradation. When strongly activated in *Xenopus* eggs, the ERK pathway induces prominent phosphorylation and SCF$^{\beta\text{-TrCP}}$-dependent degradation of Cdc25A. p90rsk, the kinase downstream of ERK, directly phosphorylates Cdc25A on multiple sites, which, interestingly, overlap with Chk1 phosphorylation sites. Furthermore, ERK itself phosphorylates Cdc25A on multiple sites, a major site of which apparently is phosphorylated by cyclin-dependent kinase (Cdk) in Chk1-induced degradation. p90rsk phosphorylation and ERK phosphorylation contribute, roughly equally and additively, to the degradation of Cdc25A, and such Cdc25A degradation occurs during oocyte maturation in which the endogenous ERK pathway is fully activated. Finally, and importantly, ERK-induced Cdc25A degradation can elicit cell cycle arrest in early embryos. These results suggest that strong ERK activation can target Cdc25A for degradation in a manner similar to, but independent of, Chk1 for cell cycle arrest.

INTRODUCTION

The Cdc25A phosphatase, a key cell cycle regulator in vertebrates, dephosphorylates and activates cyclin-dependent kinases (Cdks), thereby promoting cell cycle progression (Donzelli and Draetta, 2003). On genotoxic stress, however, the checkpoint kinases Chk1 and Chk2 hyperphosphorylate Cdc25A and target it for rapid degradation, thereby inducing cell cycle arrest for DNA repair (Bartek and Lukas, 2003). In human cells, Chk1 phosphorylation promotes the binding of β-transducing repeat-containing protein (β-TrCP), the F-box protein of the Skp1/Cullin1/F-box protein (SCF)$^{\beta\text{-TrCP}}$ ubiquitin ligase (Frescas and Pagano, 2008), to the doubly phosphorylated DSG motif (DpSGX$_{2-4}$pS) of Cdc25A and thereby targets the phosphatase for degradation (Busino *et al.*, 2003; Jin *et al.*, 2003). In *Xenopus* eggs and embryos, activated Chk1 also phosphorylates and targets *Xenopus* Cdc25A for SCF$^{\beta\text{-TrCP}}$-dependent degradation, but, in this case, by promoting the binding of β-TrCP to the nonphosphorylated DDG motif (DDGX$_2$D) (which also exists and functions in human Cdc25A) (Shimuta *et al.*, 2002; Kanemori *et al.*, 2005). In both human and *Xenopus* Cdc25A proteins, however, Chk1 phosphorylates multiple conserved Arg-X-X-Ser motifs in the N-terminal regulatory domain (Busino *et al.*, 2003; Uto *et al.*, 2004). Although phosphorylation of a conserved Ser-Pro motif is also required for the Chk1-induced degradation of human Cdc25A, the responsible kinase is not known (Busino *et al.*, 2003).

Mitogen-activated protein kinase (MAPK) pathways regulate diverse cellular processes ranging from proliferation and differentiation to apoptosis. In vertebrates, there are three major MAPK signaling pathways: extracellular signal-regulated kinase (ERK), Jun NH_2-terminal kinase (JNK), and p38 MAPK pathways (Raman *et al.*, 2007). The ERK pathway is mainly activated by mitogenic stimuli, such as growth factors and phorbol esters (Meloche and Pouyssegur, 2007). In contrast, the JNK pathway is activated by radiation and other environmental stresses, whereas the p38 pathway is activated by numerous stresses, such as UV irradiation, cytokines, and osmotic shock (Raman *et al.*, 2007). Interestingly, the p38 pathway is involved in the degradation of Cdc25A that occurs in response to UV irradiation and interleukin withdrawal in certain mammalian cells (Khaled *et al.*,

This article was published online ahead of print in *MBC in Press* (http://www.molbiolcell.org/cgi/doi/10.1091/mbc.E09-01-0008) on February 25, 2009.

Address correspondence to: Noriyuki Sagata (nsagascb@mbox.nc.kyushu-u.ac.jp or nsagascb@kyushu-u.org).

Abbreviations used: ERK, extracellular signal-regulated kinase; MAPK, mitogen-activated protein kinase; Mkp3, mitogen-activated protein kinase phosphatase 3; SCF, Skp1/Cullin1/F-box protein; Xe, *Xenopus*.

2005; Reinhardt *et al.*, 2007). This Cdc25A degradation is important for cell cycle arrest that follows, but its mechanism is poorly understood (Reinhardt *et al.*, 2007).

Whereas weak or sustained activation of the ERK pathway is generally mitogenic, its strong activation by oncogenic Ras or activated Raf causes differentiation in certain cell types and cell cycle arrest (and senescence) in many cell types (Ebisuya *et al.*, 2005; Meloche and Pouyssegur, 2007). This cell cycle arrest has been suggested to be elicited by the ERK-mediated up-regulation of negative cell cycle regulators, such as p53 and Cdk inhibitors (such as $p21^{Cip1}$ and $p16^{Ink4a}$) (Pumiglia and Decker, 1997; Serrano *et al.*, 1997; Zhu *et al.*, 1998; Meloche and Pouyssegur, 2007). Although hitherto not recognized, however, such cell cycle arrest might also be contributed to by an ERK-dependent down-regulation of some positive cell cycle regulator(s).

In this study, we have investigated whether strong ERK activation can induce down-regulation (or degradation) of the positive cell cycle regulator Cdc25A. We show that the ERK pathway, when strongly activated in *Xenopus* eggs, phosphorylates and targets Cdc25A for degradation. This degradation involves the $SCF^{\beta\text{-}TrCP}$ ubiquitin ligase and requires phosphorylations by both ERK and its downstream kinase p90rsk. Furthermore, strong ERK activation can cause cell cycle arrest in early embryos by targeting Cdc25A for degradation. These results, together with other results, suggest that, unexpectedly, the ERK pathway can target Cdc25A for degradation in a manner very similar to Chk1 and that Cdc25A degradation contributes to cell cycle arrest caused by strong ERK activation.

MATERIALS AND METHODS

Oocytes, Eggs, and Embryos

Oocytes, unfertilized eggs, and embryos were prepared, microinjected, and cultured as described previously (Kanemori *et al.*, 2005; Inoue *et al.*, 2007). Oocyte maturation and artificial egg activation were induced by progesterone (5 mg/ml) and the calcium ionophore A23187 (1 mg/ml), respectively, as described previously (Kanemori *et al.*, 2005; Inoue *et al.*, 2007). Artificially activated eggs are a very good system (for their single-cell nature) to express exogenous proteins (by mRNA injection) and to analyze regulation of cell cycle regulators, such as Cdc25A and Wee1 (Kanemori *et al.*, 2005; Okamoto and Sagata, 2007). We usually used the eggs after 40 min of artificial activation.

cDNAs and In Vitro Transcription

cDNAs encoding *Xenopus* Cdc25A, a constitutively active form of *Xenopus* p90rsk, and a dominant-negative mutant of *Xenopus* β-TrCP were described previously (Shimuta *et al.*, 2002; Kanemori *et al.*, 2005; Inoue *et al.*, 2007). cDNAs encoding mouse mitogen-activated protein kinase kinase (MKK) 1 or MAP kinase-ERK kinase (MEK) 1 (accession number NM 008927), human MKK6 (NM 002758), *Xenopus* MKK7 (NM 001087648), *Xenopus* JNKa (AB073999), human $p21^{Cip1}$ (NM 000389), and human MKP3 (NM 001946) were isolated by polymerase chain reaction (PCR) from appropriate cDNA libraries. A constitutively active form of MEK1 was made by deleting the region encompassing amino acids 32–51 and by mutating two serine residues (Ser-218→Asp, Ser-222→Glu) (Mansour *et al.*, 1994). A constitutively active form of MKK6 was made by mutating two residues (Ser-207→Asp, Thr-211→Asp) (Alonso *et al.*, 2000), whereas that of MKK7 by mutating three residues (Ser-268→Asp, Thr-272→Glu, Ser-274→Asp) (Yamanaka *et al.*, 2002). All the cDNA constructs were subcloned into either the N-terminally Myc-tagged or glutathione *S*-transferase (GST)-tagged pT7-G (UKII-) transcription vectors (Uto *et al.*, 2004; Kanemori *et al.*, 2005). In vitro mutagenesis and transcription of the cDNAs were performed as described previously (Shimuta *et al.*, 2002).

In Vitro Translation

In vitro translation of Xe-Cdc25A mRNA was performed using wheat germ extracts (L4380; Promega, Madison, WI) as described previously (Inoue *et al.*, 2007).

GST Fusion Proteins

cDNAs encoding *Xenopus* Cdc25A peptides (S36, residues 16-56; S85, 58-102; S120, 91-136; S129, 104-154; S137, 120-168; S190, 166-215; S198, 175-213; and S295, 265-316) and their Ser→Ala mutant peptides were subcloned into the pGEX-3X plasmid vector, and the GST-fused peptides were bacterially expressed and purified by standard methods.

Morpholino Oligonucleotides (Oligos)

Antisense morphlino oligos against *Xenopus* Erp1 mRNA were prepared and injected into one-cell embryos as described previously (Inoue *et al.*, 2007).

In Vitro Kinase Assays

For in vitro p90rsk and ERK kinase assays, GST-fused Xe-Cdc25A peptides were incubated with [γ-^{32}P]ATP and either p90rsk2 protein (14–480; Millipore, Billerica, MA) or ERK2 protein (P6080; New England Biolabs, Ipswich, MA) and analyzed essentially as described previously (Inoue *et al.*, 2007). In vitro translated Xe-Cdc25A protein was incubated with ERK2 protein in the absence of [γ-^{32}P]ATP as described previously (Inoue *et al.*, 2007).

Antibodies and Immunoblotting

Anti-*Xenopus* Cdc25A phospho-Ser-85 antibody was raised in rabbits against peptides (LDpSPIKMDLRC) and affinity-purified by standard methods. Routinely, proteins equivalent to one oocyte or egg were analyzed by immunoblotting using anti-*Xenopus* Cdc25A antibody (Shimuta *et al.*, 2002), anti-Myc antibody (A-14; Santa Cruz Biotechnology, Santa Cruz, CA), anti-GST antibody (Z-5; Santa Cruz Biotechnology), anti-phospho-p44/42 MAPK antibody (9106; Cell Signaling Technology, Danvers, MA), anti-phospho-JNK antibody (9251; Cell Signaling Technology), anti-phospho-p38 antibody (9211; Cell Signaling Technology), anti-Cdk1 phospho-Thr-14/Tyr-15 antibody (44–686G; BioSource International, Camarillo, CA), anti-*Xenopus* Erp1 antibody (Inoue *et al.*, 2007), or anti-*Xenopus* Cdc25A phospho-Ser-85 antibody, essentially as described previously (Uto *et al.*, 2004). In some experiments, oocyte or egg extracts before immunoblotting were treated with λ phosphatase as described previously (Inoue *et al.*, 2007).

RESULTS

Activation of ERK Induces Degradation of Xe-Cdc25A in Xenopus Eggs

First, we examined whether strong activation of ERK, p38, or JNK MAPKs could induce degradation of Cdc25A. For this, we ectopically expressed, by mRNA injection, their immediate upstream activators (MKKs) in artificially activated *Xenopus* eggs, and then monitored activating phosphorylation of endogenous MAPKs and the levels of endogenous Cdc25A (Xe-Cdc25A) by immunoblotting. Activated eggs (which mimic fertilized eggs) are a very good in vivo system to reproducibly analyze regulatory mechanisms of cell cycle regulators, such as Cdc25A and Wee1 (Kanemori *et al.*, 2005; Okamoto and Sagata, 2007; see *Materials and Methods*). Ectopic expression of a constitutively active (CA) form of MKK6, an activator of p38, efficiently induced activating phosphorylation of endogenous p38 but only very weakly induced the mobility shift and degradation of Xe-Cdc25A (Figure 1A, MKK6-CA) (see *Discussion*). Expression of a CA form of MKK7 (a JNK activator) (together with JNK; Lei *et al.*, 2002) did not induce any appreciable mobility shift or degradation of Xe-Cdc25A (Figure 1A, MKK7-CA + JNK). In contrast to these, expression of a CA form of MEK1 (or MKK1), an activator of ERK, strongly induced both mobility upshifts (due to phosphorylation; Figure 1B) and degradation of Xe-Cdc25A (Figure 1A, MEK-CA). In this experiment, however, MEK-CA expression induced activating phosphorylation of not only ERK but also JNK (Figure 1A, MEK-CA). However, JNK activation after MEK-CA expression was far much weaker than that after MKK7-CA expression, which itself could not induce any mobility shift or degradation of Xe-Cdc25A (Figure 1A, MKK7-CA + JNK). Thus, these results suggest that strong activation of the MEK/ERK pathway can specifically induce prominent phosphorylation and degradation of endogenous Xe-Cdc25A in *Xenopus* eggs.

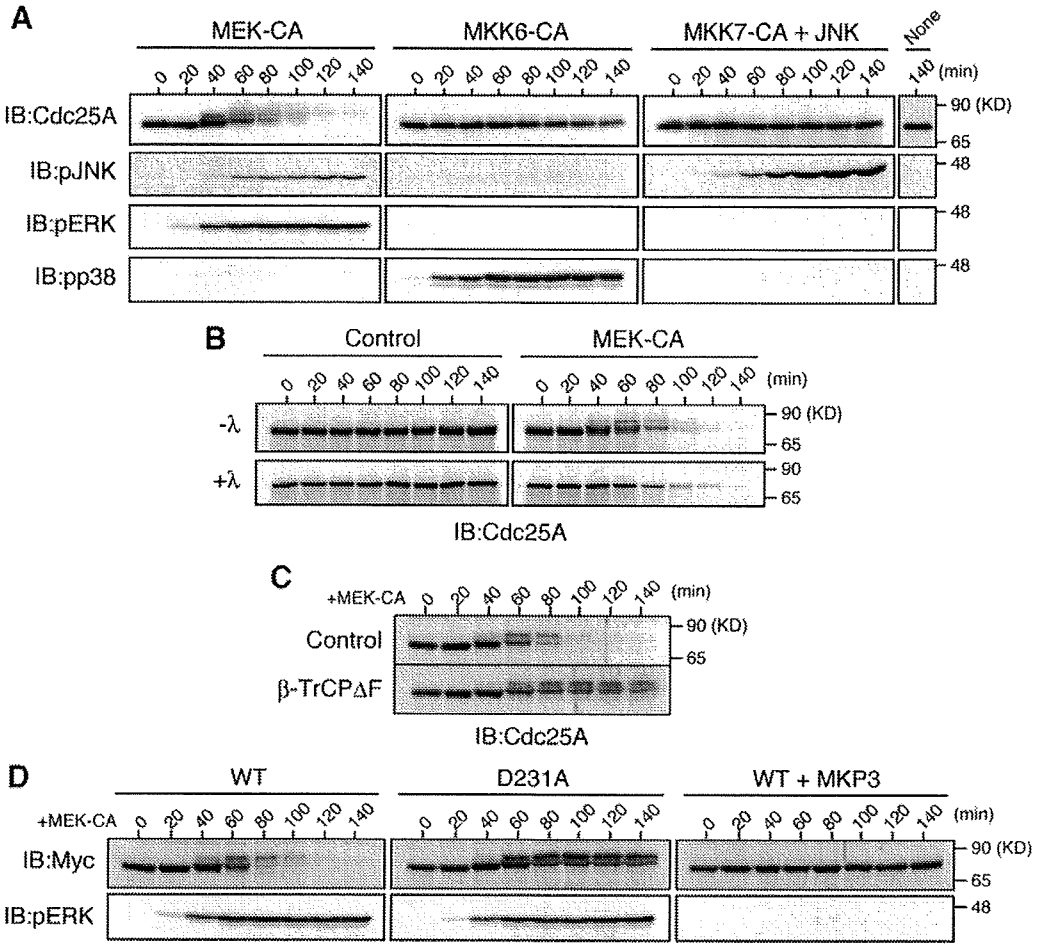

Figure 1. Induction of $SCF^{\beta\text{-}TrCP}$-dependent degradation of Xe-Cdc25A by the ERK pathway. (A) Artificially activated eggs (or eggs after 40 min of calcium ionophore treatment) were injected or not with 9 ng of JNK mRNA, reinjected 2.5 h later (time 0) with 9 ng of either MEK-CA, MKK6-CA, or MKK7-CA mRNAs, and analyzed at 20-min intervals by immunoblotting (IB) with anti-Xe-Cdc25A, anti-phospho-JNK, anti-phospho-ERK, and anti-phospho-p38 antibodies. (B) Activated eggs were injected with 9 ng of GST mRNA (Control) or MEK-CA mRNA. Egg extracts were then treated (+λ) or not (−λ) with λ phosphatase and analyzed for Xe-Cdc25A by immunoblotting. (C) Activated eggs were injected with 18 ng of GST mRNA (Control) or dominant-negative β-TrCPΔF mRNA, reinjected 2.5 h later with 9 ng of MEK-CA mRNA, and then analyzed for Xe-Cdc25A by immunoblotting. (D) Activated eggs were injected or not with 9 ng of MKP3 mRNA, reinjected 40 min later with 2 ng of mRNA encoding Myc-tagged WT or D231A Xe-Cdc25A, further injected 2.5 h later with 9 ng of MEK-CA mRNA, and then analyzed for Myc-Xe-Cdc25A constructs and phospho-ERK by immunoblotting. Five, three, four, and four independent experiments were performed for A, B, C, and D, respectively, and, for each, a typical result is shown.

Involvement of $SCF^{\beta-TrCP}$ in the ERK-induced Degradation of Xe-Cdc25A

Interestingly, the kinetics of phosphorylation and degradation of Xe-Cdc25A after MEK-CA expression (or ERK activation) in activated eggs is very similar to that after Chk1 activation in the same egg system (Shimuta *et al.*, 2002; Kanemori *et al.*, 2005). However, Chk1 itself was apparently not involved in the MEK-CA–induced phosphorylation or degradation of Xe-Cdc25A, because Chk1 was not activated at all in MEK-CA–expressing eggs (data not shown), just as in normal eggs (Shimuta *et al.*, 2002). Nevertheless, given the similar phosphorylation and degradation of Xe-Cdc25A, MEK-CA-induced Xe-Cdc25A degradation might be mediated by the $SCF^{\beta\text{-}TrCP}$ ubiquitin ligase, which is involved in Chk1-induced Xe-Cdc25A degradation (Kanemori *et al.*, 2005). To test this possibility, we overexpressed a dominant-negative mutant of β-TrCP (β-TrCPΔF) in activated eggs (Kanemori *et al.*, 2005). This treatment prevented the degradation (but not phosphorylation) of endogenous Xe-Cdc25A after MEK-CA expression (Figure 1C). Furthermore, when ectopically expressed in eggs, a Myc-tagged, Asp-231→Ala mutant of Xe-Cdc25A (D231A), i.e., the DDG motif mutant that cannot bind β-TrCP upon Chk1 activation (Kanemori *et al.*, 2005), was extremely stable even after expression of MEK-CA (Figure 1D). In these experiments, even Xe-Cdc25A WT was very stable (and apparently not phosphorylated) if MKP3, an ERK (but not MEK)-inactivating phosphatase (Muda *et al.*, 1996), was coexpressed with MEK-CA (Figure 1D). These results, together with the above-mentioned results (Figure 1A), strongly suggest that the MEK/ERK pathway, only downstream of MEK, phosphorylates Xe-Cdc25A and targets it for $SCF^{\beta\text{-}TrCP}$-dependent degradation.

Phosphorylation of Xe-Cdc25A by p90rsk and Its Contribution to ERK-induced Xe-Cdc25A Degradation

We attempted to identify the phosphorylation site(s) required for Xe-Cdc25A degradation after ERK activation.

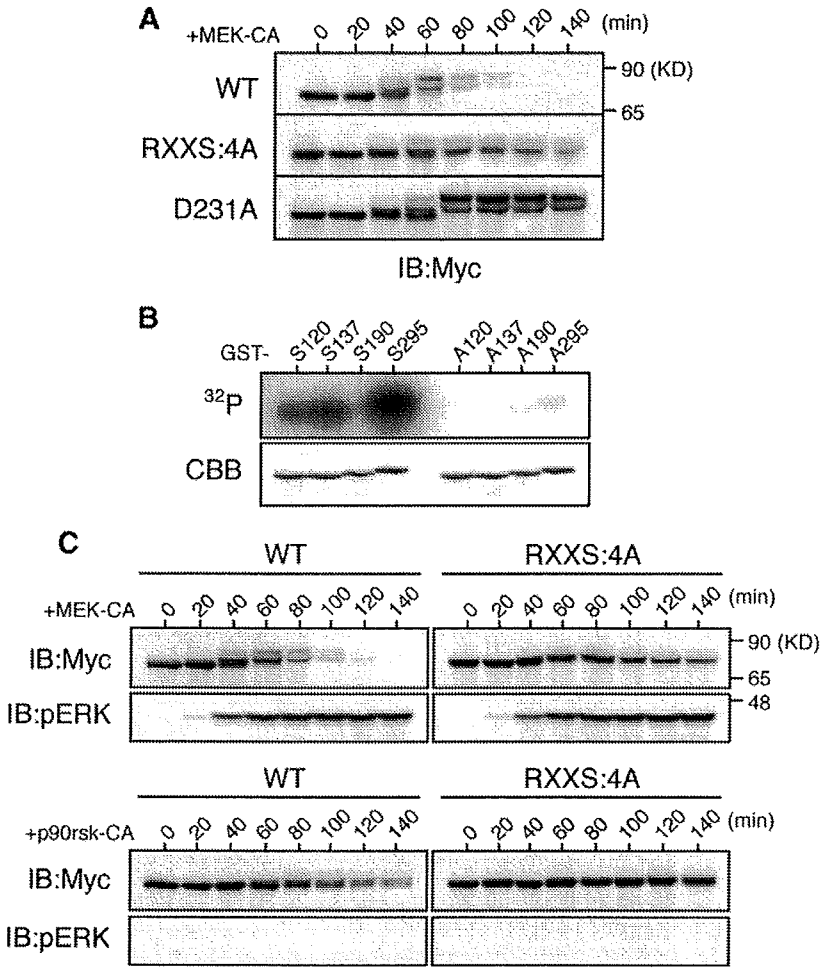

Figure 2. p90rsk phosphorylation, and its requirement for the ERK pathway-induced degradation, of Xe-Cdc25A. (A) Activated eggs were injected with 2 ng of mRNA encoding the indicated Myc-Xe-Cdc25A constructs, reinjected 2.5 h later with 9 ng of MEK-CA mRNA, and then analyzed for Myc-Xe-Cdc25A constructs by immunoblotting. (B) GST-fused Xe-Cdc25A peptides (GST-S120, GST-A120, etc., each named after the relevant Ser or substituted Ala residue numbers) were incubated with [γ-^{32}P]ATP and p90rsk protein, subjected to SDS-polyacrylamide gel electrophoresis, stained with Coomassie Brilliant Blue (CBB), and then autoradiographed (^{32}P). (C) Activated eggs were injected with 2 ng of mRNA encoding the indicated Myc-Xe-Cdc25A constructs, reinjected 2.5 h later with either 9 ng of MEK-CA mRNA or 36 ng of p90rsk-CA mRNA, and analyzed for Myc-Xe-Cdc25A constructs and phospho-ERK by immunoblotting. Four, three, and four independent experiments were performed for A, B, and C, respectively, and, for each, a typical result is shown.

Previously, we showed that phosphorylation by Chk1 of four Ser residues (S120, S137, S190, and S295) in the Arg-X-X-Ser (RXXS) motifs is required for the Chk1-induced degradation of Xe-Cdc25A (Uto *et al.*, 2004). We therefore asked whether these Ser residues would be required for ERK-induced Xe-Cdc25A degradation. When expressed in activated eggs, a Xe-Cdc25A mutant in which all of the four Ser residues were mutated to Ala (RXXS:4A) was significantly more stable than the wild type (WT), although not as stable as the completely stable D231A mutant, after MEK-CA expression (Figure 2A). Furthermore, the RXXS:4A mutant was somewhat less phosphorylated than the WT, as evidenced by its smaller size shifts, after MEK-CA expression (Figure 2A). Thus, intriguingly, the ERK pathway seems to phosphorylate at least some Chk1 phosphorylation sites for Xe-Cdc25A degradation.

We noted that, like Chk1, p90rsk, the kinase downstream of ERK (Sturgill *et al.*, 1988), belongs to the Ca^{2+}/calmodulin-regulated kinase subfamily of protein kinases and can phosphorylate RXXS motifs in its substrates (Frodin and Gammeltoft, 1999; Inoue *et al.*, 2007). We therefore first tested whether p90rsk could phosphorylate any of the four Chk1 phosphorylation sites in Xe-Cdc25A. When analyzed by in vitro kinase assays using [γ-^{32}P]ATP and GST-fused Xe-Cdc25A peptides (with or without Ala substitution), three (S120, S137, and S295) of the four Ser residues were significantly phosphorylated by p90rsk (Figure 2B). We then addressed whether ectopic expression of a constitutively active form of p90rsk (p90rsk-CA) can induce degradation of Xe-Cdc25A (WT or RXXS:4A) in activated eggs. Xe-Cdc25A WT was degraded after p90rsk-CA expression, albeit significantly less efficiently than after MEK-CA expression; notably, however, the RXXS:4A mutant was completely stable even after p90rsk-CA expression, although it was somewhat degraded after MEK-CA expression (Figure 2C). Together, these results suggest that p90rsk can phosphorylate Xe-Cdc25A on at least three Ser residues in the RXXS motifs and that this phosphorylation is required, in part, for ERK-induced Xe-Cdc25A degradation.

Phosphorylation of Xe-Cdc25A by ERK

Our observations that even the RXXS:4A mutant is somewhat degraded after MEK-CA expression (Figure 2, A and C) and that Xe-Cdc25A WT is degraded more efficiently after MEK-CA expression than after p90rsk-CA expression (Figure 2C), suggest that some other kinase(s), in addition to p90rsk, is involved in the MEK-CA-induced phosphorylation and degradation of Xe-Cdc25A. If so, the other kinase could be ERK itself, because MEK-CA expression induced a stronger phosphorylation (as well as degradation) of Xe-Cdc25A than p90rsk-CA expression (Figure 2C) and this phosphorylation (as well as degradation) was completely